NATIONAL TECHNICAL UNIVERSITY OF ATHENS

School of Naval Architecture and Marine Engineering

Examining the Effect of a Wind-Assisted Propulsion System (Flettner Rotors) on Ship's Energy Efficiency

DIPLOMA THESIS

Dimitrios Gkoufas

Supervisor: Nikolaos Themelis, Assistant Professor

Athens, February 2023

Table of Contents

List of Figures

List of Tables

Acknowledgements

The present thesis is the final requirement for the fulfillment of my studies at the School of Naval Architecture and Marine Engineering of the National Technical University of Athens.

First of all, I wish to express my sincere appreciation to my supervisor, Assistant Professor Nikolaos Themelis, for providing me with the opportunity and inspiration to explore this intriguing subject. Without his wonderful support, cooperation, and guidance this thesis would not have been possible.

Furthermore, I wish to express my gratitude to all the academic personnel and the shipping company Golden Union for the assistance and the valuable data they provided me with.

Finally, I would like to thank my friends and family, my mother, Spyridoula; my father, Vasilis; and my brother, George; for their unconditional love and support. Thank you!

List of Symbols

A	Area of the affected cross-sectional surface of the Flettner rotor
A_F	Frontal windage area
A_r	Surface area of the Flettner rotor
AWA	Apparent wind angle
C	Factor for CO_2 tons produced from 1 ton of burned fuel
C_{air}	Aerodynamic resistance coefficient
C_D	Drag coefficient
C_f	Skin friction coefficient
C_L	Lift coefficient
D	Drag force
D_P	Propeller diameter
f_{eff}	Availability factor
F_f	Frictional force
FOC	Fuel consumption
F_x	Effective force acting horizontally to the ship movement
F_y	Effective force acting vertically to the ship movement
g	Gravity acceleration
h_s	Significant wave height
J	Advance coefficient
K_Q	Open water propeller torque coefficient
K_T	Open water propeller thrust coefficient
L	Lift force
n_t	Transmission coefficient

P_{con}	Power required to rotate the rotor
P_D	Delivered power to the propeller
P_{MCR}	Ship's rated power
P_{net}	Net power output of the Flettner rotor
P_S	System power output
P_{TD}	Estimation shaft power at design draft condition
R_{air}	Aerodynamic resistance
R_{aw}	Added resistance in waves
R_{cw}	Hull resistance in calm water
Re	Reynold's number
R_{fr}	Flettner rotor's cylinder radius
SFC	Specific fuel consumption
T	Propeller Thrust
t	Thrust deduction factor
TWA	True wind angle
U_{rot}	Rotational speed of the Flettner rotor
V_a	Apparent wind speed
V_{rat}	Velocity ratio
V_{ref}	Reference velocity
V_s	Ship speed
V_t	True wind speed
w	Wake fraction
β	Apparent wind angle
γ	Angle of wind speed
η_s	Flettner rotor's system efficiency

μ_a	Air's dynamic viscosity
ρ	Seawater density
ρ_a	Air density
ω	Flettner rotor's cylinder rotational speed

Abstract

Due to the increasing urgency for decarbonization in the maritime industry, wind-assisted cargo ships have the potential to play a crucial role in achieving the IMO 2050 goal of reducing the total annual GHG emissions from international shipping. The purpose of this thesis is to contribute knowledge on the performance of Rotor Sails on commercial vessels, which are widely considered as a leading Wind-Assisted Propulsion System (WASP). The operating principles of the Flettner rotor are analyzed and a set of Matlab codes is developed and utilized to generate results related to the rotor's energy aspects, with the ultimate aim of determining the Energy Efficiency Design Index (EEDI).

This research presents and compares the EEDI results under various wind conditions, as well as for rotors with diverse mechanical properties, thereby providing a deeper understanding of the energy capabilities of Flettner rotors. The findings from this research indicate that the results of the power propulsion of the rotor are significantly influenced by its dimensions, mechanical and structural properties, as well as the wind conditions encountered by the vessel. Based on the aforementioned outcomes, recommendations are being made regarding the optimization of calculating the efficiency of Flettner rotors.

Lastly, a case study is carried out for a bulk carrier equipped with 4 rotor sails to evaluate the EEDI through two separate methodologies. Initially, the original method proposed by the IMO for calculating EEDI is employed and then another methodology is utilized, which involves a series of calculations to determine the total propeller thrust of the vessel and ultimately calculate the power required from the engine. The results of this case study outline the significance of wind conditions as well as the impact of the forces exerted by wind and waves, not only on the Flettner rotors but on the vessel as a whole.

Περίληψη

Τα εμπορικά πλοία με συστήματα πρόωσης αιολικής υποβοήθησης δύνανται, λόγω της επιτακτικής ανάγκης για μείωση των εκπομπών CO_2 στον τομέα της διεθνής ναυτιλίας, να λάβουν ένα κρίσιμο ρόλο στην επίτευξη του στόχου του IMO 2050 για την ελαχιστοποίηση των συνολικών ετήσιων εκπομπών GHG. Σκοπός της παρούσας διπλωματικής εργασίας είναι η διάχυση γνώσης σχετικά με την απόδοση των Rotor Sails στα εμπορικά πλοία, τα οποία θεωρούνται ευρέως ως κορυφαίο σύστημα πρόωσης αιολικής υποβοήθησης (WASP). Αρχικά περιγράφονται και αναλύονται οι αρχές λειτουργίας του ρότορα Flettner, ενώ στην συνέχεια αναπτύσσεται ένα σύνολο κωδίκων Matlab. Οι κώδικες αυτοί χρησιμοποιούνται για τη παράθεση αποτελεσμάτων σχετικά με την ενεργειακή αποδοτικότητα του ρότορα, με απώτερο σκοπό τον προσδιορισμό του Δείκτη Σχεδιασμού Ενεργειακής Απόδοσης (EEDI).

Με τη παρούσα έρευνα στόχος είναι η αναφορά και η σύγκριση των αποτελεσμάτων EEDI υπό διάφορες συνθήκες ανέμου, καθώς και τα αποτελέσματα για ρότορες με διαφορετικές μηχανικές ιδιότητες, παρέχοντας έτσι μια βαθύτερη κατανόηση των ενεργειακών δυνατοτήτων των ρότορων Flettner. Τα ευρήματα αυτής της έρευνας αποδεικνύουν ότι η ισχύς πρόωσης του ρότορα επηρεάζεται σημαντικά από τις διαστάσεις του, τις μηχανικές και δομικές του ιδιότητες, καθώς και από τις συνθήκες ανέμου που συναντά το πλοίο. Επομένως, έχοντας ως γνώμονα τα παραπάνω πορίσματα αλλά και περεταίρω συγκρίσεις αποτελεσμάτων, μπορούν να διατυπωθούν προτάσεις σχετικές με τη βελτιστοποίηση του υπολογισμού της απόδοσης των ρότορων Flettner.

Ακολούθως, πραγματοποιείται μια μελέτη για ένα φορτηγό πλοίο εξοπλισμένο με 4 Rotor Sails και σκοπό την αξιολόγηση του EEDI μέσω δύο διαφορετικών μεθοδολογιών. Αρχικά, χρησιμοποιείται η μέθοδος που προτείνεται από τον IMO και μετέπειτα μια μεθοδολογία απαρτιζόμενη από υπολογισμούς για τον προσδιορισμό της συνολικής πρόωσης της έλικας του πλοίου με απώτερο σκοπό τον υπολογισμό της ισχύος που απαιτείται από τον κινητήρα. Τα αποτελέσματα αυτής της μελέτης τονίζουν τη σημασία των δυνάμεων που προκαλούνται από τον άνεμο και τα κύματα, στους ρότορες Flettner αλλά και στο πλοίο.

1 Introduction

1.1 Background

As the world continues to grapple with the COVID-19 pandemic, the pressing issue of climate change remains an ongoing concern that requires attention. To mitigate the effects of climate change, countries have committed to reducing their greenhouse gas emissions through the Paris Agreement, which aims to limit global warming to below 2ºC and pursue efforts to limit it to 1.5ºC. One sector that is particularly significant in this effort is the maritime transport industry, which emits approximately 1,076 million tonnes of CO_2 annually and accounts for 2.89% of global greenhouse gas emissions according to the 4th IMO GHG study [1]. To address this, the International Maritime Organization (IMO) has set a goal to reduce total annual GHG emissions by at least 50% by 2050 and to eventually phase them out entirely. This has led ship owners and operators to explore alternative and more sustainable propulsion systems.

One promising green technology that is gathering renewed interest is wind propulsion, an age-old concept with a modern twist. For centuries, wind power was used to transport cargo across the globe, until it was replaced by steam and diesel during the industrial era. Wind propulsion involves the use of devices such as rotor sails, wing sails or soft sails to harness the energy of the wind and generate forward thrust. Contemporary aeronautical technology has been integrated into these devices to make them more efficient than traditional sails. Wind power is an easily accessible and renewable energy source at sea, and can drive ships directly without any energy losses. The implementation of weather routing can also play a crucial role in boosting performance and savings [2], [3]. These wind propulsion devices can also be retrofitted to existing ships as an auxiliary power source, known as wind-assisted propulsion. Research and designs are currently focusing on making wind propulsion the primary power source for vessels. However, this research project primarily concentrates on wind propulsion in conjunction with another main power source.

As a result of the increasing fuel prices and the potential shortage of fossil fuel, research on wind propulsion has once again gained momentum following the industrial revolution. One of the wind-assisted propulsion systems that were developed during the 20th century was the rotor sails. The history of Rotor sails, also known as Flettner rotors, dates back to the 1920s when German engineer Anton Flettner began experimenting with the concept of using large cylindrical rotors as a means of wind propulsion for ships [4]. Despite early success, interest in rotor propulsion technology faded in the 1930s due to the advent of more efficient diesel engines and the economic downturn. However, in recent decades, with the increasing focus on decarbonization, wind-assisted propulsion systems like Flettner rotors are being considered as a green alternative for the merchant shipping industry to reach environmental targets and save costs. Leading companies such as Norsepower and Anemoi Marine are now focusing on developing these sorts of technologies [5], [6]. Other wind-assisted propulsion systems such as the DynaRig, kites, Turbosail, and Rigid Wing Sails have been also under constant development and research

over the 20th and 21st centuries [7], [8]. Although these are very interesting wind-assisted propulsion alternatives, this thesis primarily concentrates on rotor sails.

1.2 Aim and Objectives

Although the wind has been utilized in maritime transport for centuries, there is a significant gap in understanding the effectiveness of wind-assisted cargo ships. More research is needed to determine the true potential of wind propulsion and to provide reliable data on the cost-benefit of this technology. In order to increase confidence in wind-assisted propulsion systems, validated information must be obtained to accurately predict fuel savings and cost reductions.

Thus, the aim of this thesis is to expand knowledge regarding the performance of Rotor Sails on commercial vessels. To accomplish this, a calculation framework for ships with retrofitted rotor sails is developed. One of the key features of this framework is that it requires minimal input data and the mechanical abilities of the rotor sails can be highly adaptable. In simpler terms, it is an easy-to-use tool that can predict the performance, such as the EEDI index, of any commercial ship with rotor sails on board, using generic input data such as vessel main particulars and rotor sail dimensions, with a reasonable level of accuracy and low computational time.

Therefore, the objectives of the research are the following ones:

- Researching about the working principle and the underlying physics of the Rotor Sails.
- Develop a methodology outlining the data inputs and procedures for predicting the EEDI index.
- Creating a calculation framework that predicts the performance of ships with retrofitted Rotor Sails using simplified models, known as semi-empirical methods, that rely on a combination of experimental data and theoretical calculations, to minimize the amount of input data needed and decrease the computational time.
- Comparing the performance between different configurations of the WASP system.
- Conducting a case analysis of a ship equipped with Flettner rotors and determining the Energy Efficiency Design Index (EEDI) through two distinct methodologies.
- Identifying potential challenges and limitations associated with the use of rotor sails on commercial vessels.

In chapter 2, the fundamental operating principle of rotor sails is introduced and the primary sailing functions of rotor sails are described. Moreover, the significance of rotor sails as an innovative technology is highlighted through the listing of several noteworthy vessels that have been retrofitted with rotor sails.

In chapter 3, the method and computational procedure for determining the EEDI index for a vessel with and without Flettner rotors, as well as for varying Flettner rotor configurations, are presented. A comparison of the results is then performed, and conclusions are drawn from the findings.

Lastly, in chapter 4, a case study is conducted on a ship equipped with Flettner rotors, where the EEDI index is calculated using two distinct methodologies. Furthermore, some of the operational limitations of Flettner rotors that were not considered in chapter 3 are demonstrated, and a comparison of the results obtained through the two methodologies is presented.

1.3 Literature Review

Previous chapters have highlighted the urgent need for action to address climate change, and the importance of rapid action to avoid dangerous levels of climate change. One potential solution to decarbonize the shipping sector is to incorporate wind-assisted propulsion systems into the international shipping fleet. Of the various modern wind-assisted propulsion systems, known as WASP systems, rotor sails seem to be the most promising. Although these WASP systems are mostly still in the research and development phase, some shipping companies have already implemented rotor sails on a few of their vessels [9]–[12]. This chapter reviews relevant literature on wind-assisted propulsion systems and focuses specifically on rotor sails.

In Nikos Vasileiadis's publication [13], with the help of his professor Stephen Salter, a study aiming to analyze the propulsion system of a Marine Cloud Brightening (MCB) vessel is presented. MCB is a remote-operated ship that releases submicron drops of seawater to increase the reflectivity of clouds to solar energy [14]. The propulsion system of the ship is achieved by using vertical Flettner rotors, while the energy for the sprays is generated by using alternating pitch-variation hydrofoils. The research examines the forces and powers produced by the MCB spray vessel propulsion system, which is composed of two Flettner rotors, and also determines the power generated from the hydrofoils, which is required to rotate the rotors and produce the spray. The research provides insight into the performance and efficiency of the propulsion system of the MCB vessel.

Figure 1: The Marine Cloud Brightening vessel (MCB) [15]

One noteworthy aspect of Vasileiadis's research is the methodology used to calculate the forces produced by the Flettner rotors and the power output of the system. A Python code was created to calculate the power output of the cylinder, using only basic data inputs for a specific Flettner rotor design, making it accurate and efficient in terms of computation time. This method allows for easy and fast prediction of the performance of the Flettner rotor. The results for the lift and drag coefficient were obtained from experimental data produced by Ackeret [16], which were found to be in good agreement with the theoretical predictions. This methodology provides an understanding of how the rotor behaves in different wind conditions and allows for the prediction of the system's performance in different scenarios.

Moreover, a profile of the net power output is presented for each fixed rotational speed of the rotor ranging from 100 to 1000 rpm, enabling the assessment of the efficiency of the rotor at different speeds. This information is crucial in the design and optimization of the rotor sails. The methodology used in this research allows for a better understanding of the physics behind the Flettner rotor and the performance of the propulsion system on the MCB vessel.

Reche's master's thesis focuses on the development of a Performance Prediction Program for wind-assisted cargo ships in order to contribute to the knowledge of the performance of this technology [17]. The program is able to predict the performance of three types of Wind-Assisted Propulsion Systems (WAPS): Rotor Sails, Rigid Wing Sails, and DynaRigs.

The program is characterized by its generic structure, the small number of input data required, and its ability to predict the performance of ships with these WAPS installed. The program balances the forces and moments predicted by the hull and WAPS models

in 6 degrees of freedom to predict the theoretical sailing performance of the wind-assisted cargo ship under various wind conditions. The program allows different optimization objectives to be considered, such as maximizing sailing speed or total power savings.

A model validation is carried out to evaluate its reliability, comparing the results with real sailing data of a Long Range 2 (LR2) class tanker vessel, the Maersk Pelican, which was recently fitted with two 30-meter high Rotor Sails and results from another performance prediction program. In general, the results from the two performance prediction programs and some of the real sailing measurements show good agreement. However, for some downwind sailing conditions, the performance predictions are more conservative than the measured values. The findings of the study show that Wind-Assisted Propulsion Systems have a high potential in playing a key role in the decarbonization of shipping.

Besides the effects Flettner rotors have on the different wind conditions, another aspect that needs to be mentioned is the interaction between two or more rotating cylinders with each other. Through the utilization of wind-tunnel experimentation, Bordogna was able to investigate the aerodynamic effects resulting from the interaction of two rotating cylinders [18]. The results of the study indicate that the performance of Flettner rotors is sensitive to their location on the deck as well as their relative positioning to one another. The greatest effects were observed when the cylinders were situated in close proximity and aligned with the direction of the wind. Furthermore, the arrangement of the forward thrust-producing hardware shows a significant impact on the useful forces produced and the heeling angles of the ship. However, it should be noted that in this research, the positioning of the Flettner rotors has not been taken into account.

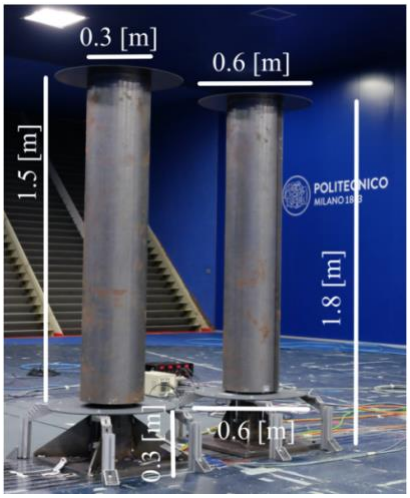

Figure 2: The experimental Flettner rotors used for Bordogna's thesis [18]

In conclusion, the research presented above has highlighted the potential of Flettner rotors as a viable alternative for ship propulsion. In the following chapters, through the combination of methodologies inspired by literature, we have been able to calculate the effective thrust forces and power outputs of a single Flettner rotor and subsequently, the

EEDI index. This has allowed us to compare the results and further solidify the attractiveness of Flettner rotors as a solution for decarbonization in the shipping industry.

1.4 Regulatory Framework of the EEDI

The Energy Efficiency Design Index (EEDI) is a mandatory international regulatory framework established by the International Maritime Organization (IMO) to reduce the carbon emissions of ships and promote more energy-efficient vessel design [19]. The EEDI sets minimum energy efficiency standards for new ships and requires ship operators to demonstrate compliance with these standards.

The basic principle of the index is given below:

$$EEDI = \left(\frac{gr}{ton-mile}\right) = \frac{FOC*C}{Capacity*Vs} \rightarrow \frac{CO_2\ emissions \rightarrow cost\ of\ society}{Work \rightarrow profit\ of\ society} \quad 1.1$$

Where:

- FOC: fuel consumption
- C: factor for CO_2 tons produced from 1 ton of burned fuel and the value depends on the type of fuel
- Capacity: Deadweight
- Vs: Vessel speed

The unified EEDI calculation formula is presented in the following Figure 3:

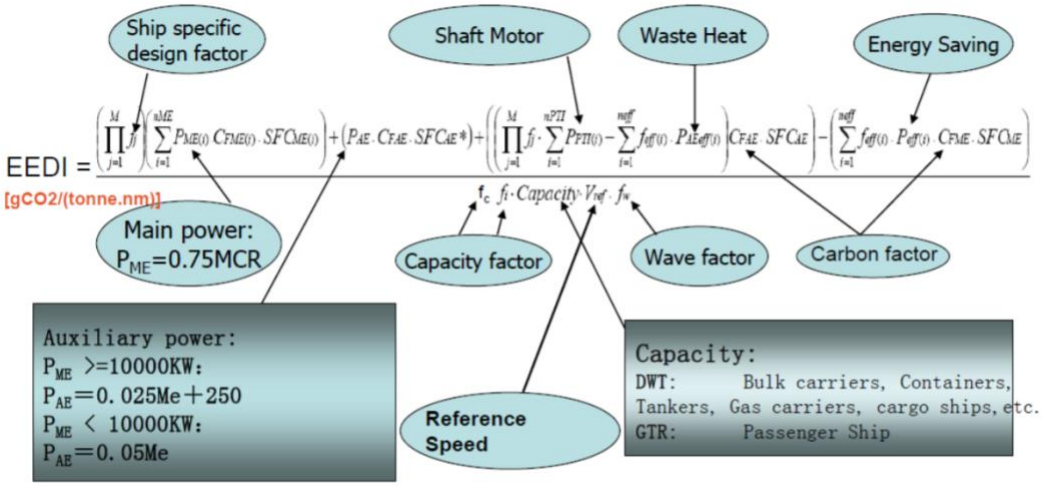

Figure 3: Integrated EEDI calculation formula [20]

Where in Table 1 below all the parameters and their descriptions are displayed.

Table 1: Description of the EEDI parameters

Capacity	[tonne]	The deadweight capacity in summer draft
$\mathbf{C_{FAE}}$	[g CO_2 / g fuel]	Factor for CO_2 produced from burned fuel of the auxiliary engines
$\mathbf{C_{FME}}$	[g CO_2 / g fuel]	Factor for CO_2 produced from burned fuel of the main engine
$\mathbf{f_{eff}}$	[-]	Availability factor of innovative energy efficiency technology
$\mathbf{f_i}$	[-]	Capacity factor for any technical / regulatory limitation on capacity
$\mathbf{f_c}$	[-]	Cubic capacity correction factor (for chemical tankers and gas carriers)
$\mathbf{f_j}$	[-]	Correction factor to account for ship-specific design elements (e.g. ice classed ships, shuttle tankers)
$\mathbf{f_w}$	[-]	Non-dimensional coefficient indicating the decrease of speed in representative sea condition of wave height, wave frequency and wind speed
$\mathbf{n_{eff}}$	[-]	Number of innovative technologies
$\mathbf{n_{ME}}$	[-]	Number of main engines
$\mathbf{n_{PTI}}$	[-]	Number of power addition systems
$\mathbf{P_{ME}}$	[kW]	75% of the main engine MCR considering the existence of shaft motor of shaft generator
$\mathbf{P_{AE}}$	[kW]	Auxiliary engine power
$\mathbf{P_{AEeff}}$	[kW]	Auxiliary power reduction due to innovative electrical energy efficient technology
$\mathbf{P_{eff}}$	[kW]	Output of innovative mechanical energy efficient technology for propulsion at 75% main engine power
$\mathbf{P_{PTI}}$	[kW]	75% of rated power consumption of shaft motor
$\mathbf{SFC_{AE}}$	[g / kW]	Certified specific fuel consumption for auxiliary engines
$\mathbf{SFC_{ME}}$	[g / kW]	Certified specific fuel consumption for main engine
$\mathbf{V_{ref}}$	[knots]	Ship speed at reference conditions

The EEDI framework is divided into three phases, with increasingly stringent requirements for new ships in each phase [21]. The first phase started in 2013 and the third phase will start in 2025. Reduction factors (X) will be used to implement the EEDI in phases to gradually reduce the required EEDI. The required EEDI will be reduced by X % every five years based on the initial value (Phase 0) and depending on the vessel size [22]. The EEDI phases are:

1. Phase 0 (1 Jan. 2013 – 31 Dec. 2014) – 0 %
2. Phase 1 (1 Jan. 2015 – 31 Dec. 2019) – 10 %
3. Phase 2 (1 Jan. 2020 – 31 Dec. 2024) – 15 % and 20 % (depends on the ship type)
4. Phase 3 (1 Jan. 2025 – onwards) – 30 %

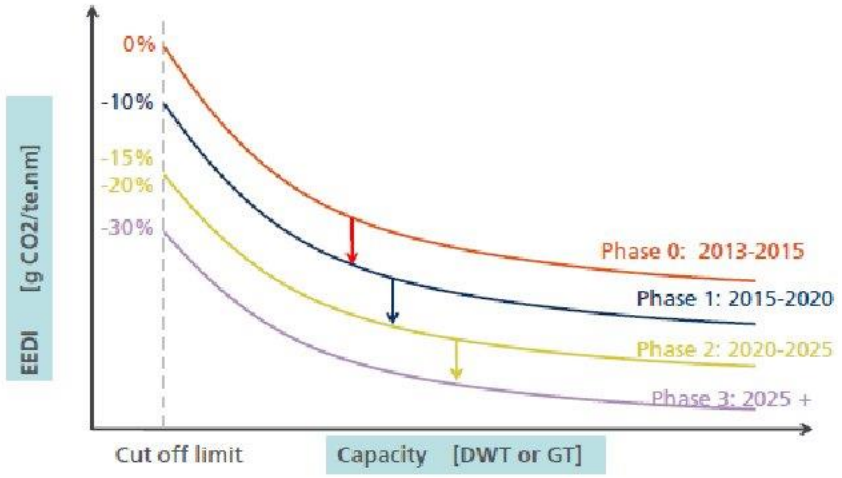

Figure 4: Phases for reduction factor of EEDI [22]

1.4.1 IMO Classification of Wind-Assisted Propulsion Systems

Wind-assisted propulsion systems, such as sails or kites, can be an effective way to reduce a ship's energy consumption and emissions. Therefore, the IMO allows ships equipped with these systems to be eligible for reduced EEDI requirements. However, the exact regulations and requirements for wind-assisted propulsion systems under the EEDI framework vary depending on the specific type of system and the ship's operating profile [23]. According to the International Maritime Organization (IMO), wind-assisted propulsion systems, such as Flettner rotors, are considered innovative energy efficiency technologies. These systems fall under the category of "Reduction of Main Engine Power" and specifically in Category B-2, which allows them to be treated separately from the overall performance of the vessel [20].

Innovative Energy Efficiency Technologies				
Reduction of Main Engine Power			Reduction of Auxiliary Power	
Category A	*Category B-1*	*Category B-2*	*Category C-1*	*Category C-2*
Cannot be separated from overall performance of the vessel	Can be treated separately from the overall performance of the vessel		Effective at all time	Depending on ambient environment
	$f_{eff}=1$	$f_{eff}<1$	$f_{eff}=1$	$f_{eff}<1$
– low friction coating – bare optimization – rudder resistance – propeller design	– hull air lubrication system (air cavity via air injection to reduce ship resistance) (can be switched off)	– wind assistance (sails, Flettner-Rotors, kites)	– waste heat recovery system (exhaust gas heat recovery and conversion to electric power)	– photovoltaic cells

Figure 5: Classification of Innovative Energy Efficiency Technologies [23]

1.4.2 IMO Proposals and Amendments on Wind-Assisted Propulsion Systems (WASP)

The International Maritime Organization (IMO) has proposed new regulations for wind-assisted propulsion systems in order to promote their use and reduce the carbon emissions of ships. These systems, which include sails and kites, have the potential to significantly improve ship's energy efficiency and reduce its environmental impact. The IMO's proposals can be made by a variety of stakeholders, including government agencies, ship operators, shipbuilders, and other industry groups. The IMO's Member Governments, which are countries that have joined the organization, are also able to make proposals. All the proposals are considered by the IMO's Marine Environment Protection Committee (MEPC) and Technical Committee (TC) and if accepted will be developed into draft regulations to be adopted by the IMO member states.

The findings on the EEDI assessment framework for wind propulsion systems submitted by China, also identifiable from the document's name "MEPC 74/INF.39" [24], yielded particularly noteworthy findings in regard to the Hard Airfoil Sailing Project. As evidenced in the document, the wind propulsion system's contribution to the EEDI reduction below the baseline is minimal, at only 1.6%. However, when considering a specific subset of routes on which the vessel frequently operates and neglecting the global wind probability matrix that the IMO suggests, the percentage of EEDI reduction below the baseline increases dramatically to 35.5%, with a contribution of 16% from the wind propulsion system.

The information presented in the document MEPC 74/INF.39 [24], specifically the Hard Airfoil Sailing Project, suggests that if the EEDI calculation for ships is based on a global wind probability matrix, the actual energy-saving benefits of wind-assisted propulsion systems will be underestimated. This could lead to a decrease in ship owners' willingness to invest in these systems, which is not in line with the IMO's goal of encouraging the use of new energy-efficient and emission-reducing technologies in the maritime industry.

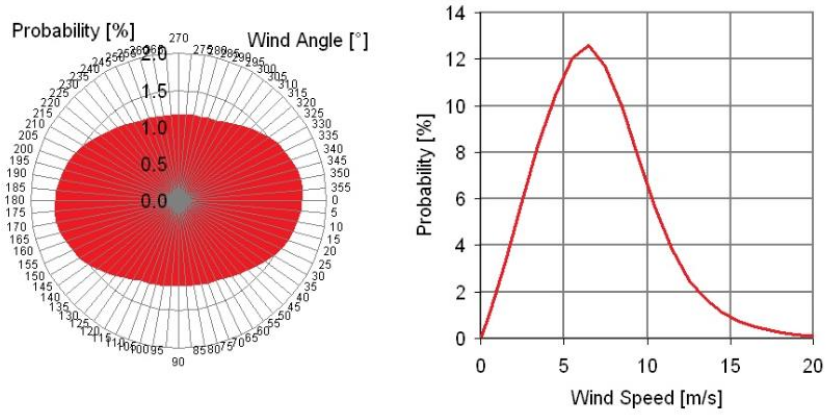

Figure 6: Resulting wind curves on the main global shipping routes relative to the ship [25]

The above idea was also introduced in the document MEPC 79/INF.21 titled as "Reduction of GHG Emissions from Ships", submitted by Comoros, Finland, France, Saudi Arabia, Solomon Islands, Spain, RINA, and IWSA [26]. The examination of a wind-assisted Panamax bulk carrier fitted with 4 rotor sails revealed that the percentage of carbon intensity reduction between two voyages, one without voyage optimization and one utilizing it, resulted in a 22.3% and 27.8% decrease respectively. This is a substantial decrease in carbon intensity, but it should be noted that with the implementation of more advanced weather routing and speed adjustments thus increasing voyage time, an even greater reduction in carbon intensity could be achieved.

It is noteworthy that while there have been numerous proposals and amendments to the "2013 Guidance on Treatment of Innovative Energy Efficiency Technologies for Calculation and Verification of the Attained EEDI" document, also known as MEPC.1/Circ.815 [20], there have been relatively few changes made to the newly revised 2021 MEPC.1/Circ.896 document [23]. The primary goal of this revision is to provide greater clarity in regard to the procedures for calculating the available effective power of the system, thus reducing the potential for misunderstandings or errors in the definitions and calculation process.

Furthermore, in the latest version of "Guidance on Treatment of Innovative Energy Efficiency Technologies for Calculation and Verification of the Attained EEDI" MEPC.1/Circ.896 [23], it is worth mentioning some of the procedures and limitations regarding wind-assisted propulsion systems. One of the instructions for calculating the wind propulsion system force matrix is considering the reference height of the WASP. Specifically, according to the IMO, in order to calculate the relative wind velocity an extrapolation of the wind speed to the reference height of the WASP must be made. However, in this study the reference height is not considered as there are no experimental data on the vessel's loading condition and it is insignificant based on the IMO's suggested formula:

$$V_{ref} = V_{10m}\left(\frac{z_{ref}}{10}\right)^{a} \quad 1.2$$

Where z_{ref} is the reference height above the water line and it is defined as the mid-height of the Flettner rotor, V_{10m} is the wind velocity at 10 m above sea level, V_{ref} is the resulting wind velocity at the reference height and α is set to 1/9 in accordance with ITTC guidelines.

In line with the IMO guidance, it is necessary for every developer of wind-assisted propulsion systems to be offering the structural design files of the product. In order to meet operational requirements for all wind directions and forces, it is important to consider not only the wind direction and force but also the total forces generated by the wind-assisted propulsion system, including lateral forces on the vessel and yawing moments.

2 Introduction of Rotor Sails

Humans have been utilizing the energy of wind for centuries, with early examples of sailing ships dating back to ancient Egypt and the Mediterranean. However, it is believed that the Austronesian people were the first to develop specialized maritime technology for sea travel, as early as 3000 BC. Despite the long history of sailing and ships, the underlying physics can be complex. This chapter aims to provide a basic understanding of the physical principles behind rotor sails and key concepts that will be necessary for a comprehensive understanding of this thesis.

2.1 Wind Velocity Triangle

The energy source for rotor sails, as well as traditional sails, is the power of the wind. The propulsion generated by sails is produced by the apparent wind, which is the relative airflow experienced by an observer in motion. The absolute value of the wind is the result of combining the velocity of the headwind and the true wind velocity. In other words, it is the vector sum of the true wind velocity minus the speed of the vessel.

As a ship increases its speed, the apparent wind magnifies, and its point of origin shifts forward. This is the wind that crew members on board feel and what the sails encounter as inflow. When a ship reduces its speed, the apparent wind tends to be identical to the true wind. The true wind is an external factor, which remains constant despite the ship's speed.

The relationship between true wind, ship sailing speed, and apparent wind forms the fundamental concept of the wind velocity triangle.

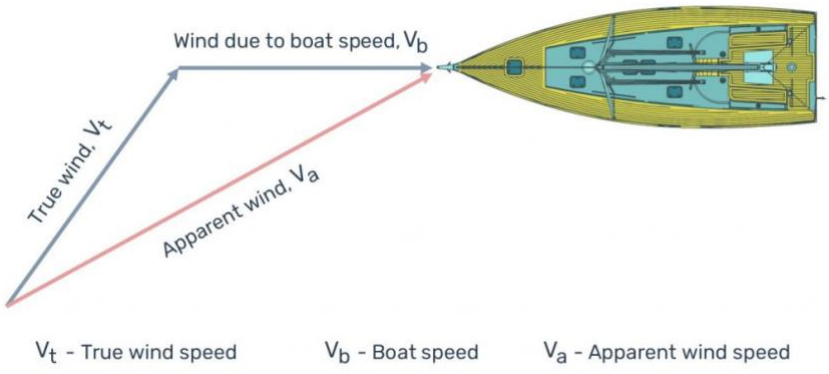

Figure 7: Simplified Wind Velocity Triangle [27]

2.2 Magnus Effect

The lifting force generated by rotor sails is attributed to the phenomenon known as the Magnus effect, named after Gustav Magnus, a Professor of Physics at the University of Berlin from 1834 to 1869. This effect is well-known for its impact on the trajectory of a spinning object moving through a fluid and is also present in various ball games such as football and tennis. In the case of a rotating cylinder, the Magnus effect can be understood as the superposition of two simple flows, a parallel flow, and a circulatory flow as can be seen in Figure 8. The resulting flow pattern is determined by the sum of the free-stream parallel flow velocity, V_{free}, and the circulatory flow, $V_{rotating}$. The streamlines moving in the direction of the flow created by the Rotor, V_{favour}, have a total velocity of:

$$V_{favour} = V_{free} + V_{rotating} \quad 2.1$$

While, the streamlines moving against have a total velocity, $V_{against}$, of:

$$V_{against} = V_{free} - V_{rotating} \quad 2.2$$

The Magnus effect results in a velocity difference between the two sides of the rotating cylinder, leading to a pressure distribution across the device, as described by Bernoulli's theorem, "where the velocity increases, the pressure diminishes." The lack of symmetry between the upper and lower sides of the cylinder results in the manifestation of a lifting force, which pushes the cylinder towards the side of lower pressure.

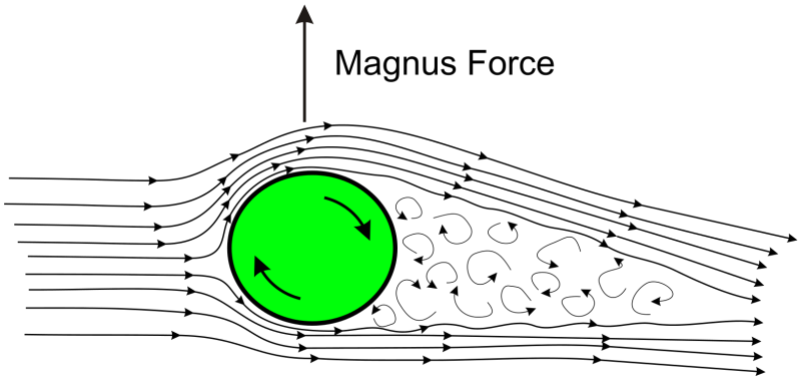

Figure 8: The Magnus Effect exhibited in a rotating cylinder, where the vertical arrow symbolizes the lift force generated [28]

2.3 Rotor Sails in Contemporary Shipping

In the 21st century, an increasing number of vessels are incorporating innovative technologies in order to decrease their EEDI/EEXI and adhere to IMO guidelines. Some of the notable vessels that have employed rotor sail technology include:

- The RoLo (roll-on/lift-off) cargo ship E-Ship 1 was developed by ENERCON and was launched in August 2008. Four 27x4 meter Rotor Sails were installed, with Enercon, the third-largest wind turbine manufacturer, claiming operational fuel savings of up to 25% compared to similar conventional freight vessels [29].
- In 2018, the Maersk Pelican became the first product tanker fitted with two 30x5 meter Norsepower Rotor sails. The constructor, Norsepower, confirmed fuel savings of 8.2% and a corresponding reduction in CO2 emissions in the Maersk Pelican project [9].
- In 2018, the M/V Afros, a vessel owned by the Greek shipping company Blue Planet Shipping Ltd., became the first bulk carrier fitted with rotor sails by ANEMOI. Four Rotor Sails, each measuring 16x2 meters, were installed and the company estimates a reduction of fuel consumption and emissions of 12.5% [12].

As seen from the examples above, all Rotor Sail developers report promising performance from this application of the Magnus effect for commercial use. There are numerous advantages to implementing Rotor Sail systems on cargo ships, most notably fuel savings and associated cost reductions. One misconception is that using rotor sails necessitates an increase in crew size, which is not the case. In fact, little to no specialized training is required for operating these devices, as their performance is mainly monitored. Additionally, Rotor Sails require lower costs for installation and maintenance per unit of thrust force than other wind-assisted propulsion systems.

From a navigational perspective, Rotor Sails offer exceptional maneuverability. The ship can be directed forwards or backwards, depending on the direction of rotation, and can be moved laterally without altering course due to its lateral force. Another notable characteristic of Rotor Sails is their inherent load limit; as all rotating cylinders have a maximum operating speed, they will decrease their velocity and aerodynamic loads at high wind speeds. This self-regulating feature makes them resistant to hurricanes, unlike other types of wind-assisted propulsion systems. However, it is important to consider the vibrations generated by Rotor Sails and ensure that they fall within acceptable limits to prevent crew discomfort or damage to the ship's structure. Additionally, it should be noted that, unlike other wind-assisted propulsion systems, Rotor Sails require energy to operate. This power consumption will be taken into account when comparing the performance of different wind-assisted propulsion systems. Lastly, one of the main concerns for shipping companies regarding the adoption of this technology was the difficulty in loading and unloading cargo at ports due to the height and volume of the rotor sails. Solutions such as foldable units or units that can retract into the cargo area have been developed to address this issue.

3 Methodology and Results

3.1 Calculation of the vessel's reference velocity

Figure 9 incorporates the entire calculation process into a flowchart representation.

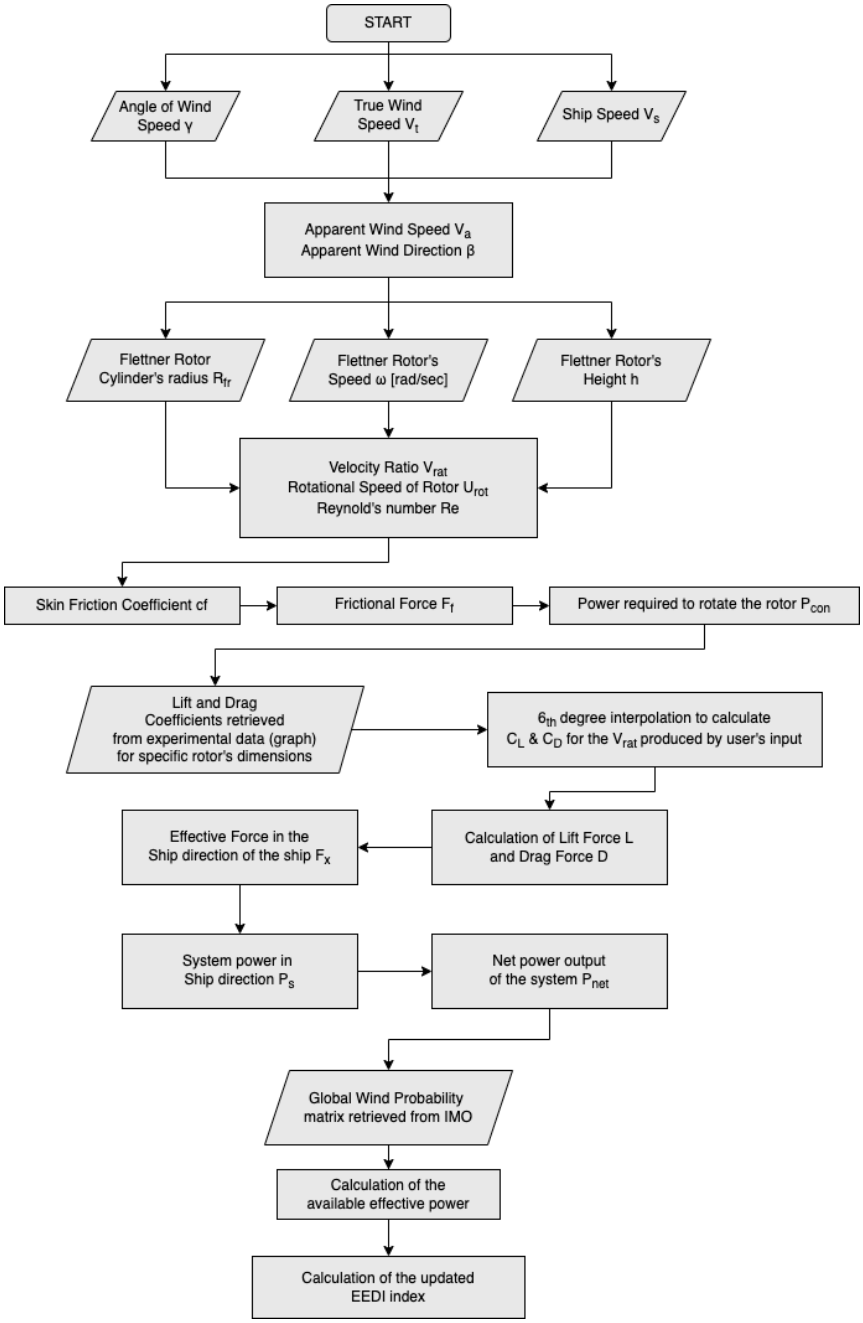

Figure 9: Flowchart of Matlab code used for calculating the EEDI index

3.1.1 Vessel's main particulars

For the purpose of this case study, we will be using a bulk carrier as the vessel of reference. Table 2 presents some of the most basic and important particulars about this vessel:

Table 2: Ship's Main Particulars

Length between Parallels LBP	222 [m]
Breadth B	38 [m]
Design draught T_d	12.5 [m]
Design displacement	89506 [tons]
P_{MCR} Main Engine	13506 [kW]
Type of fuel (ME)	HFO
Type of fuel (AE)	Diesel Oil

3.1.2 Calculation of reference speed

In order to determine the energy efficiency of a ship, it is necessary to estimate the velocity of the ship at its design draft condition while operating at 75% of its rated power [30]. This information can be obtained by collecting data points from the "Sea Trial Measurement Report" of the studied vessel. Specifically, by analyzing a table that provides an estimation of the velocity corresponding to the power at design load condition, it is possible to calculate the reference Velocity, V_{ref}.

Table 3: Estimation of power at design load condition

Speed (kn)	**P_{TD} (kW)**
14.5	8747
15	9720
15.5	10878
16	12158

From a simple script on Matlab, with the data set of Table 3, a quadratic polynomial function is generated as shown in Figure 10 below:

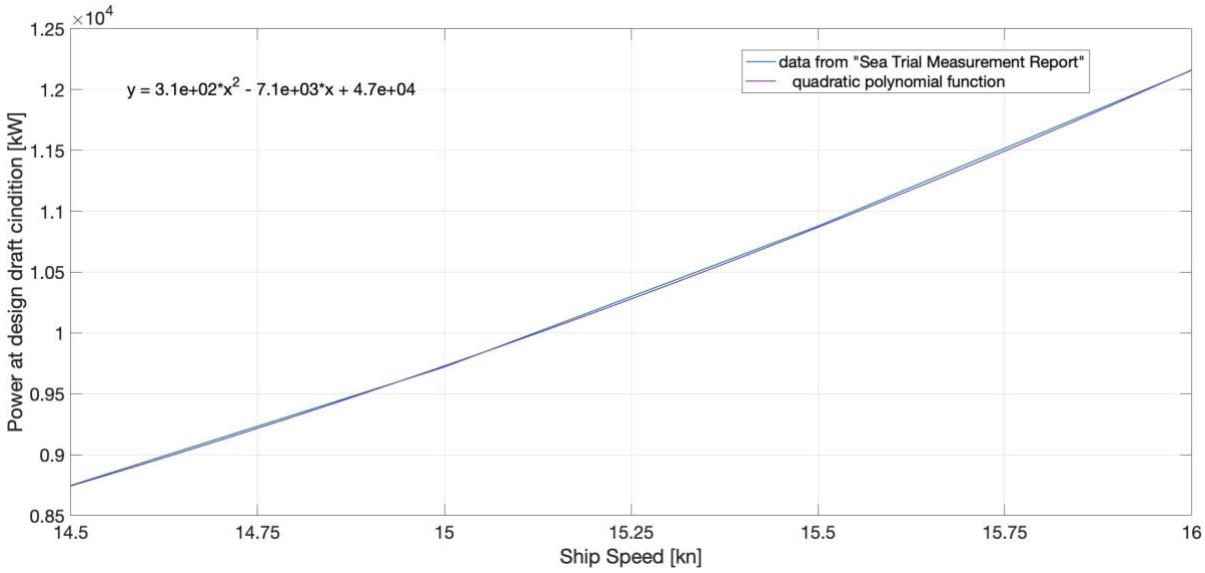

Figure 10: Plot of Matlab's script about the reference Velocity

From Figure 10, the quadratic polynomial function that is being generated is the following:

$$P_{TD} = 307 \cdot V^2 - 7.09 \cdot 10^3 \cdot V + 4.69 \cdot 10^4 \quad 3.1$$

Where P_{TD} is measured in kW and V in knots.

Solving the above quadratic function with "y=75%MCR=10170 kW" as a given value, the V_{ref} is equal to 15.25 knots.

3.2 EEDI Calculation of Vessel without Flettner rotor

3.2.1 Introduction of the EEDI index

During the design and construction of a vessel, it is important to calculate the EEDI index, which describes the design energy efficiency of the ship. This index is checked based on reference values that are specific to the type of ship and its capacity. The EEDI calculation is important because it helps to ensure that the ship is as energy-efficient as possible, which can reduce its environmental impact and save on operating costs. By considering the reference values, the shipbuilders and designers can make sure that the ship they are building meets the regulatory standards and will be able to operate efficiently. For the calculation of the EEDI index of a Vessel without a Flettner rotor, the following equation will be needed.

$$EEDI = \frac{f_j \cdot P_{ME} \cdot C_{FME} \cdot SFC_{ME} + P_{AE} \cdot C_{FAE} \cdot SFC_{AE}}{f_c \cdot f_i \cdot Capacity \cdot f_w \cdot V_{ref}} \quad 3.2$$

3.2.2 Calculations

To find the EEDI index first the basic characteristics of the bulk carrier that is being studied are necessary and are listed in Table 2: Ship's Main Particulars.

Emissions from the Main Engine are defined based on a specific power, which is at P_{ME}=0.75*MCR = 10170 kW. That is, one operating point of the Main Engine is considered.

Since the installed power is MCR= 13560 kW > 10000 kW, the auxiliary power is calculated based on the relationship: P_{AE} = 0.025*MCR + 250 = 589 kW

Specific Fuel Consumption (SFC):

For the main engine, it is calculated at 75% of the load, while for the auxiliary (AE) at 50% of the load. Therefore, from Table 4 it is given that SFC_{ME}= 170 gr/kWh and SFC_{AE}= 202.95 gr/kWh

The carbon factor for HFO and Diesel Oil fuel is equal to 3.114 t-CO_2/t-Fuel and 3.206 t-CO_2/t-Fuel respectively.

Table 4: Specific Fuel Consumption of Main & Auxiliary Engines on different loads

Load (%)	**SFC ME (gr/kWh)**	**SFC AE (gr/kWh)**
25	195	214.5
50	184.5	202.95
75	170	187
100	174.5	191.95

Velocity reference (V_{ref}):

That velocity has been calculated in chapter 3.1.2 thoroughly through "The Sea Trial Measurement Report" and it is equal to V_{ref} = 15.25 knots.

EEDI Calculation:

From all the data above the achieved EEDI index is calculated as:

$$\text{EEDI} = \frac{1*(10170*3.114*170)+(589*3.206*202.95)+0+0}{1*1*89506*1*15.25} = 4.225\ [\text{g} - \text{CO}_2/\text{ton} - \text{mile}] \quad 3.3$$

3.3 Calculation of Apparent wind characteristics

To initially approach the complex problem of Flettner rotors installed on the deck of the vessel, a mathematical model will be employed using Matlab software to calculate the effective forces produced by the rotor. Prior to this stage, it is essential to determine the apparent wind speed and direction for a range of true wind speeds and angles. The model is tested for a specific Flettner rotor design, with the cylinder dimensions considered as a radius of R_{fr}=1.2 m and height H=20 m. Additionally, the Flettner rotor's rotational speed ω is varied from 0 to 1000 rpm with a step of 100 rpm, although in this stage of the study, a fixed value of 500 rpm will be considered to simplify the analysis.

The apparent wind speed V_a and the apparent wind direction β at 10 meters above the sea level can be calculated through the below equations:

$$V_a = \sqrt{V_t^2 + V_s^2 - 2V_tV_s\cos(\gamma + \pi)} \quad 3.4$$

$$\beta = \cos^{-1}\left(\frac{V_t^2 - V_s^2 - V_a^2}{-2V_aV_s}\right) \quad 3.5$$

Where V_t is the true wind speed, V_s is the reference speed of the vessel and γ is the true wind direction of the ship (Figure 11).

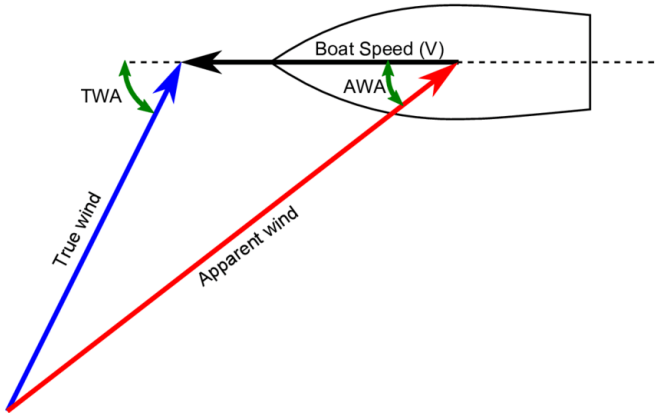

Figure 11: Wind Velocity Triangle in Sailing [31]

To comprehend the physical significance of the aforementioned equation, it is necessary to establish the conventions for positive/negative wind direction. In the present study, it is assumed that 0º represents a headwind, and 180º represents a tailwind blowing from the stern to the fore of the vessel. By utilizing these equations and a simple Matlab model, two matrices can be generated for apparent wind speed and direction, assuming a fixed value for the rotor's rotational speed, as shown in Table 5 & Table 6 below:

Table 5: Apparent Wind Speed

TRUE WIND SPEED M/S	1	6	11	16	21
TUE WIND ANGLE DEG					
0	8.844	13.844	18.844	23.844	28.844
45	8.580	12.809	17.451	22.249	27.119
90	7.907	9.875	13.510	17.819	22.417
135	7.171	5.565	7.778	11.834	16.419
180	6.844	1.844	3.156	8.156	13.156
225	7.171	5.565	7.778	11.834	16.419
270	7.907	9.875	13.510	17.819	22.417
315	8.580	12.809	17.451	22.249	27.119

Table 6: Apparent Wind Angle

TRUE WIND SPEED M/S	1	6	11	16	21
TRUE WIND ANGLE DEG					
0	0.000	0.000	0.000	0.000	0.000
45	4.727	19.343	26.469	30.565	33.199
90	7.266	37.414	54.509	63.885	69.519
135	5.659	49.700	89.518	107.052	115.257
180	0.000	0.000	180.000	180.000	180.000
225	5.659	49.677	89.518	107.052	115.257
270	7.266	37.414	54.509	63.885	69.519
315	4.727	19.343	26.469	30.565	33.199

3.3.1 Cases of different angles of attack

This section aims to evaluate various scenarios of wind direction in order to comprehend the physical meaning of the model and ensure its validity. The apparent wind, which is the wind experienced by an observer, is the relative velocity of the wind in relation to the observer. The value of the apparent wind speed and angle depends on the values of true wind speed and angle but also on the V_{ref} (vessel speed) that it is been already calculated in chapter 3.1.2.

3.3.1.1 When the True Wind Angle (TWA) is 0°

In the case of the True Wind Angle being 0°, which means the wind is coming from ahead, the apparent wind or the wind that the vessel is experiencing will be the absolute sum of the true wind speed and V_{ref}. And this is precisely what the values of the matrix (Table 7) below are presenting if V_{ref} will be transposed from knots to m/s (V_{ref} =7.8436 m/s).

Table 7: Apparent Wind Speed at 0º

TRUE WIND SPEED M/S	**1**	**6**	**11**	**16**	**21**
TRUE WIND ANGLE DEG					
0	8.844	13.844	18.844	23.844	28.844

In terms of the apparent wind angle, it is easy to comprehend that the angle of attack will be in the same direction as the true wind angle as equation 3.5 shows in chapter 3.3.

Table 8:Apparent Wind Angle at 0º

TRUE WIND SPEED M/S	**1**	**6**	**11**	**16**	**21**
TRUE WIND ANGLE DEG					
0	0.00	0.00	0.00	0.00	0.00

The values of Table 8 are considered to be all 0 despite a numerical error for some values of wind speed.

3.3.1.2 When the True Wind Angle (TWA) is 180°

In the case of the True Wind Angle being 180°, which means there is a downwind, the apparent wind, or the wind that the vessel, will heavily depend on the true wind speed and the correlation between apparent and true wind speed. Using mathematical terms, the results that will be produced are the absolute subtraction of apparent and true wind speed. That can be also seen from the following results.

Table 9: Apparent Wind Speed at 180º

TRUE WIND SPEED M/S	1	6	11	16	21
TRUE WIND ANGLE DEG					
0	6.844	1.844	3.156	8.156	13.156

In terms of the apparent wind angle, the aforementioned is changing value between 0° and 180°depending on the condition that if the value of true wind speed is less than the V_{ref}, then the wind is coming from ahead (0°, because it operates against the vessel direction), and if the value of wind speed is greater than the V_{ref}, then the wind is coming from behind (180°, because it operates with the vessel direction).

Table 10: Apparent Wind Angle at 180º

TRUE WIND SPEED M/S	1	6	11	16	21
TRUE WIND ANGLE DEG					
0	0.00	0.00	180.00	180.00	180.00

3.3.2 Conclusions about the Apparent wind

The above procedure can be followed for every possible combination of true wind speed and angle, and produce the corresponding results, but for reasons of simplicity, we will not analyze any more cases. Furthermore, it is important to note that a symmetry exists between 0°-180° and 180°-360°, thus for many of the following results the range of apparent wind angle is being deduced to 0°-180°.

3.4 Calculation of the power consumed by the rotor

After the calculation of the apparent wind, it is needed to calculate the frictional force from the air that resists the rotation of the Flettner rotor based on the flowchart from Figure 9.

Through the data from chapter 3.3, the velocity ratio V_{rat}, the linear speed of the rotor U_{rot} and the Reynold's number Re can be calculated through the below equations:

$$V_{rat} = \frac{\omega \cdot R_{fr}}{V_a} \quad 3.6$$

$$U_{rot} = \omega \cdot R_{fr} \quad 3.7$$

$$Re = \rho \cdot \omega \cdot R_{fr}^2 \cdot \frac{1}{\mu_\alpha} \quad 3.8$$

In the above equations, ρ is the air density and μ_α is the air's dynamic viscosity. The last two variables are taken from this point on and forward as 1.225 kg/m^3 and 1.81*10^{-5} kg/(m*s) for an air temperature of 15 °C. The frictional force F_f in N can be estimated via the following equation:

$$F_f = \frac{1}{2} \cdot C_f \cdot \rho \cdot U_{rot}^2 \cdot A_r \quad 3.9$$

Where A_r is the surface area of the cylinder (rotor) and C_f is the skin friction coefficient, calculated through:

$$C_f = \frac{0.0576}{Re^{1/5}} \quad 3.10$$

The power required to rotate the rotor is calculated below. However, it has to be stated that this is an approximation since factors such as the endplate and the bearing friction are not considered. If we considered these variables the power would increase and it would not be entirely dependent on friction force and the linear speed of the rotor.

$$P_{con} = F_f \cdot U_{rot} \quad 3.11$$

As it is aforementioned for this simple case we generate results for only one rotational speed, so the U_{rot} will be a fixed value as well as the F_f.

For a rotational speed of 500 rpm and after all the necessary calculations, the model generated the below value for the consumed power:

$$P_{con} = 60103\ N * \left(\frac{m}{s}\right) = 60.1\ kW \quad 3.12$$

3.5 Calculation of Lift & Drag Forces of the rotor

As the Flettner rotor rotates, a lift force is created via the Magnus effect. Along that, a drag force acts perpendicular to the Lift force and parallel to the apparent wind direction. These lift and drag forces can be calculated in N, by the below equations:

$$L = \frac{1}{2} \cdot \rho \cdot V_a^2 \cdot A \cdot C_L \quad 3.13$$

$$D = \frac{1}{2} \cdot \rho \cdot V_a^2 \cdot A \cdot C_D \quad 3.14$$

where A=48 m^2 is the area of the affected cross-sectional surface, V_a stands for the apparent wind speed the results of which are already mentioned in chapter 3.3 and the coefficients C_L and C_D refer to the lift and drag forces respectively, and they are dependent on the velocity ratio [16]. Data of these coefficients were produced for the specific model and were limited to a maximum of V_{rat}=8 as shown in Figure 12 below:

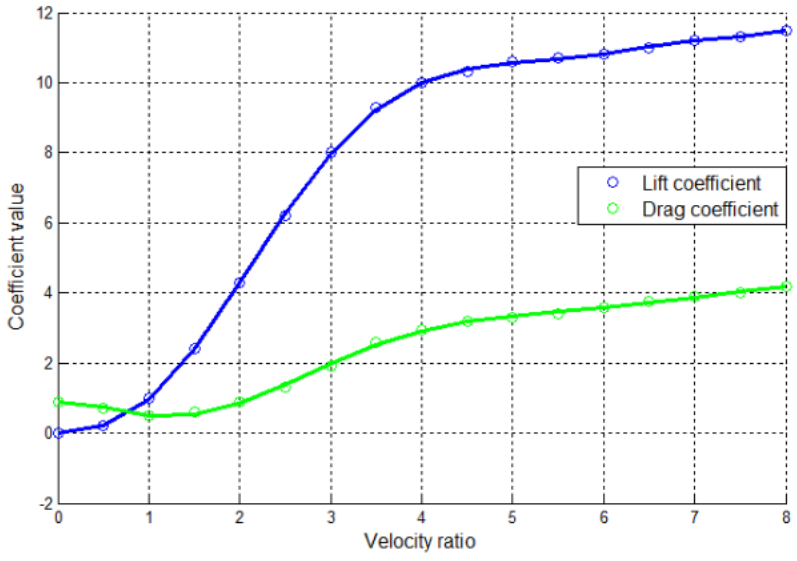

Figure 12: Values for Lift and Drag Coefficients [32]

To incorporate the data of Figure 12 into the current model, two 6th degree functions were generated (for both C_L and C_D coefficients) with the assistance of Matlab and numerical analysis. Although it is important to note that for values greater than V_{rat}=8 the coefficients are not affected by the functions as it is considered that the coefficients tend to be a constant value.

3.5.1 Results of Lift and Drag coefficients

To generate the results of Lift and Drag coefficients firstly it is important to state the two 6th degree functions.

$$C_L = -0.0008259x^6 + 0.01494x^5 - 0.05744x^4 - 0.3346x^3 + 2.405x^2 - 1.075x + 0.05456 \quad (3.15)$$

$$C_D = -0.0007167x^6 + 0.01705x^5 - 0.01437x^4 - 0.4656x^3 + 0.2084x^2 - 0.5551x + 1.025 \quad (3.16)$$

Where x is the velocity ratio with a range of 0 to 8.

The results of the Lift and Drag coefficients are presented in Table 11 & Table 12 respectively:

Table 11: C_L Coefficient

TRUE WIND SPEED M/S	1	6	11	16	21
TUE WIND ANGLE DEG					
0	11.693	10.614	8.727	6.652	5.018
45	11.828	10.825	9.331	7.274	5.527
90	11.876	11.246	10.692	9.174	7.206
135	11.834	11.834	11.834	10.951	9.758
180	11.834	11.834	11.834	11.952	10.764
225	11.834	11.834	11.834	10.951	9.758
270	11.876	11.246	10.692	9.174	7.206
315	11.828	10.825	9.331	7.274	5.527

Table 12: C_D Coefficient

TRUE WIND SPEED M/S	1	6	11	16	21
TUE WIND ANGLE DEG					
0	3.869	3.338	2.397	1.632	1.164
45	3.912	3.482	2.663	1.841	1.298
90	3.880	3.718	3.389	2.591	1.817
135	3.854	3.854	3.854	3.579	2.866
180	3.854	3.854	3.854	3.937	3.438
225	3.854	3.854	3.854	3.579	2.866
270	3.880	3.718	3.389	2.591	1.817
315	3.912	3.482	2.663	1.841	1.298

As can be seen from the results of Table 11 and Table 12 a trend exists on both matrices of coefficients, the lesser the value of wind speed is the greater the generated coefficient value. This is a logical result because smaller wind speed values correspond to a bigger velocity ratio as described by the V_{rat} equation in chapter 3 and thus the bigger coefficient values as both of these functions are considered increasing.

3.5.2 Results of Lift and Drag Forces

It is important to note that the results of Table 13 & Table 14 are the absolute values of drag and lift forces in Newton with orientation based on the apparent wind direction.

Table 13: Lift Forces

TRUE WIND SPEED M/S	1	6	11	16	21
TUE WIND ANGLE DEG					
0	26887.211	59804.358	91108.044	111177.469	122728.268
45	25598.766	52219.489	83547.847	105864.940	119505.569
90	21830.443	32242.754	57374.005	85637.422	106469.757
135	17893.813	10774.277	21051.177	45089.405	77337.755
180	16295.194	1182.561	3466.366	23376.887	54777.461
225	17893.813	10774.277	21051.177	45089.405	77337.755
270	21830.443	32242.754	57374.005	85637.422	106469.757
315	25598.766	52219.489	83547.847	105864.940	119505.569

Table 14: Drag Forces

TRUE WIND SPEED M/S	1	6	11	16	21
TUE WIND ANGLE DEG					
0	8895.1231	18809.8902	25025.7788	27282.4211	28463.8769
45	8467.1829	16797.2378	23839.0225	26790.1145	28056.0850
90	7131.0998	10659.1596	18185.8431	24187.1272	26848.8897
135	5827.9548	3509.1458	6856.2978	14734.5851	22713.5491
180	5307.2899	385.1563	1128.9836	7701.0407	17497.3195
225	5827.9548	3509.1458	6856.2978	14734.5851	22713.5491
270	7131.0998	10659.1596	18185.8431	24187.1272	26848.8897
315	8467.1829	16797.2378	23839.0225	26790.1145	28056.0850

3.6 Calculation of Flettner rotor's Power

To calculate the final power output of the system, it is needed the effective force F_x, acting horizontally to the vessel's motion, which is calculated in N.

$$F_x = L \cdot \sin\beta - D \cdot \cos\beta \quad (3.17)$$

The system power in the ship direction can be calculated in Watts, as the horizontal force acting on the ship's motion F_x multiplied by the ship's speed V_S:

$$P_S = F_x \cdot V_S \quad (3.18)$$

The net power output of the system, P_{net}, is calculated through the Matlab model via the equation below and is represented as the difference between the power offered by the rotors minus the power needed to overcome air friction. This difference is multiplied by the system's efficiency which for this case it is assumed that $\eta_s = 0.75$.

$$P_{net} = (P_S - P_{con}) \cdot \eta_S \quad (3.19)$$

3.6.1 Power output system's results

Firstly, it is important to show the results of effective force F_x in Newtons without any modification.

Table 15: F_x effective force

TRUE WIND SPEED M/S	1	6	11	16	21
TUE WIND ANGLE DEG					
0	-8895.123	-18809.890	-25025.779	-27282.418	-28463.875
45	-6328.672	1446.849	15898.275	30765.847	41958.610
90	-4312.972	11123.718	36156.103	66248.092	90345.390
135	-4035.219	5943.635	20992.764	47427.988	79635.853
180	-5307.290	-385.156	1128.984	7701.041	17497.320
225	-4035.219	5943.635	20992.764	47427.988	79635.853
270	-4312.972	11123.718	36156.103	66248.092	90345.390
315	-6328.672	1446.849	15898.275	30765.847	41958.610

As can be seen above, there are some values of the matrix are negatives, which means that the power output will be negative for the specific wind speed and orientation. So, in order to ensure maximum energy efficiency the negative values of the matrix are getting zero, therefore for these values the Flettner rotor stops operating. Important to note that this modification is not necessary as the negative values will be filtered in later stages of the procedure.

Table 16: F_x effective force corrected

TRUE WIND SPEED M/S	1	6	11	16	21
TUE WIND ANGLE DEG					
0	0.000	0.000	0.000	0.000	0.000
45	0.000	1446.849	15898.275	30765.847	41958.610
90	0.000	11123.718	36156.103	66248.092	90345.390
135	0.000	5943.635	20992.764	47427.988	79635.853
180	0.000	0.000	1128.984	7701.041	17497.320
225	0.000	5943.635	20992.764	47427.988	79635.853
270	0.000	11123.718	36156.103	66248.092	90345.390
315	0.000	1446.849	15898.275	30765.847	41958.610

After the calculation of the corrected effective force, the model can generate the results of the system's power P_S and the final net power output of the system P_{net} in Watts.

Table 17: System Power Output

TRUE WIND SPEED M/S	1	6	11	16	21
TUE WIND ANGLE DEG					
0	0.000	0.000	0.000	0.000	0.000
45	0.000	11348.504	124699.708	241314.995	329106.555
90	0.000	87249.994	283594.011	519623.535	708633.099
135	0.000	46619.499	164658.839	372006.166	624631.775
180	0.000	0.000	8855.296	60403.883	137241.975
225	0.000	46619.499	164658.839	372006.166	624631.775
270	0.000	87249.994	283594.011	519623.535	708633.099
315	0.000	11348.504	124699.708	241314.995	329106.555

Table 18: Net Power Output

TRUE WIND SPEED M/S	1	6	11	16	21
TUE WIND ANGLE DEG					
0	0.000	0.000	0.000	0.000	0.000
45	0.000	0.000	48447.592	135909.057	201752.727
90	0.000	20360.306	167618.319	344640.462	486397.635
135	0.000	0.000	78416.940	233927.435	423396.642
180	0.000	0.000	0.000	225.723	57854.292
225	0.000	0.000	78416.940	233927.435	423396.642
270	0.000	20360.306	167618.319	344640.462	486397.635
315	0.000	0.000	48447.592	135909.057	201752.727

The results of the system's power output P_{net} are considered logical. It is noticeable that a symmetry exists between 0°-180° and 180°-360°, because of the Flettner rotor's capabilities to spin both ways. Moreover, it is outlined that the highest values of power output exist on 90° with a possible deviation of ±45°. In a future model, the deviation will be much smaller (±5° deviation) but nonetheless the highest power output exists around the 90° range of wind direction.

Pnet					
	1	6	11	16	21
0	0	0	0	0	0
45	0	0	48447.5919	135909.057	201752.727
90	0	20360.3061	167618.319	344640.462	486397.635
135	0	0	78416.9402	233927.435	423396.642
180	0	0	0	225.722716	57854.2919
225	0	0	78416.9402	233927.435	423396.642
270	0	20360.3061	167618.319	344640.462	486397.635
315	0	0	48447.5919	135909.057	201752.727

Figure 13: Visualization of Net Power Output using Excel's color scaling format

The results that were presented in chapters 3.3 to 3.6.1 were generated using the assistance of the Matlab software. Specifically, the Matlab code developed to produce the above is attached to Appendix I.

3.7 EEDI Calculation of Vessel with one Flettner rotor

To calculate the new EEDI index it is necessary to first estimate the available effective power of the wind propulsion system. The available effective power of wind propulsion systems as innovative energy-efficient technology is calculated by the following formula:

$$(f_{eff} \cdot P_{eff}) = \left(\frac{0.5144 \cdot V_{ref}}{\eta_T} \sum_{i=1}^{m} \sum_{j=1}^{n} F(V_{ref})_{i,j} \cdot W_{i,j} \right) - \left(\sum_{i=1}^{m} \sum_{j=1}^{n} P(V_{ref})_{i,j} \cdot W_{i,j} \right) \quad 3.20$$

Where:

- $(f_{eff} \cdot P_{eff})$ is the available effective power delivered by the specified wind propulsion system. f_{eff} and P_{eff} are not differentiated in the calculation because availability and power are included in the global wind matrix and wind propulsion system force matrix addressing each wind condition with a probability and a specific wind propulsion system force.
- V_{ref} is the ship reference speed measured in nautical miles per hour (knot), as defined in the EEDI calculation guidelines.

- η_T is the total efficiency of the main drive(s) at 75 % of the rated installed power (MCR) of the main engine. η_T shall be set to 0.7 if no other value is specified and verified by the verifier, according to Germanischer Lloyd, the German classification society [33].
- $F(V_{ref})_{i,j}$ is the force matrix of the respective wind propulsion system for a given ship speed V_{ref}. The $F(V_{ref})_{i,j}$ matrix shall be provided by the applicant.
- $W_{i,j}$ is the global wind probability matrix.
- $P(V_{ref})_{i,j}$ is a matrix with the same dimensions as $F(V_{ref})_{i,j,}$ and $W_{i,j}$ and represents the power demand in kW for the operation of the wind propulsion system.
- The factor 0.5144 represents the conversion factor from nautical miles [nm] to meters per second [m/s].

3.7.1 Calculation of available effective power of WASP

Following the same procedures as those from chapters 3.3 - 3.6 with some necessary additions, a final value of effective power (WASP) can be generated. This procedure is taking place through a Matlab code, which will be attached to the end of the thesis.

3.7.1.1 Additions from the previous chapters

This is now a fully dynamic system where all the kinematic parameters are variables with a certain range (except for the reference speed of the vessel, which must be a constant for the calculation of EEDI). To be more specific the cylinder dimensions remain the same but the rotational speed of the Flettner rotor ω in rad/sec has a range of 100 – 1000 rpm with a step of 100 rpm.

Moreover, the new matrices must facilitate a wider and more detailed range of true wind speed and angle due to the fact that the global wind probability matrix ($W_{i,j}$) which is an official matrix from IMO and has additional and more detailed probabilistic values for more wind scenarios [23].

The new range of true wind speed is from 1 to 25 m/s with a step of 1 m/s and a true wind angle of 0° to 355° degrees with a step of 5° degrees.

3.7.1.2 Results of the P_{con} and P_s from 100 RPM to 1000 RPM

P_{con} is the power required to rotate the rotor and it is plotted in Figure 14 for the different rotor's speeds starting from 100 RPM and reaching 1000 RPM. The procedure for calculating the power consumed by the motor is referenced in chapter 3.4.

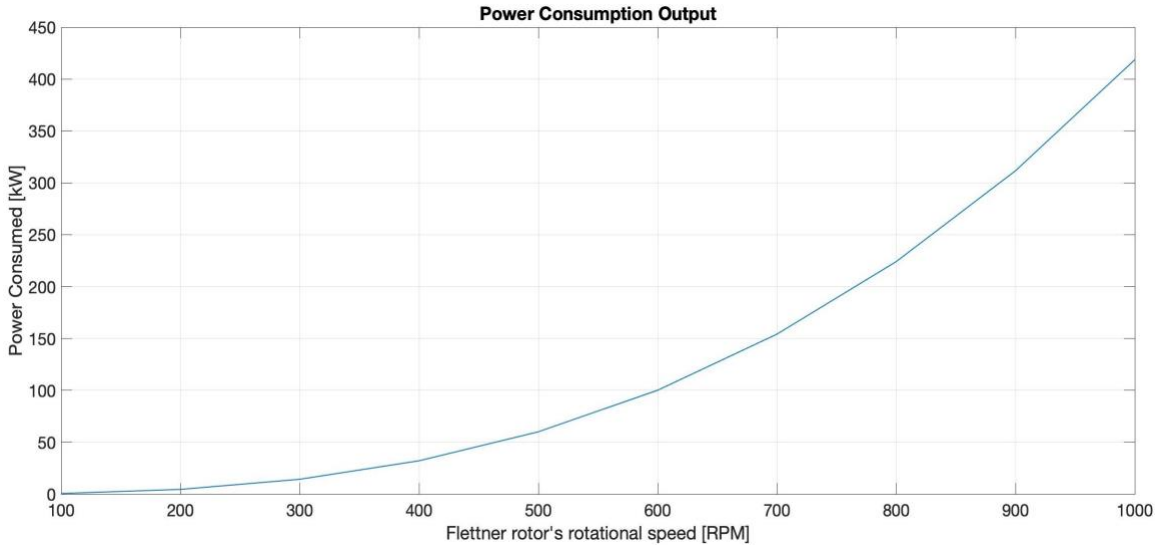

Figure 14: Power Consumption Output

P_s is the system power output and in Figure 15 the maximum power output is plotted for the different rotor's speeds starting from 100 RPM and reaching 1000 RPM.

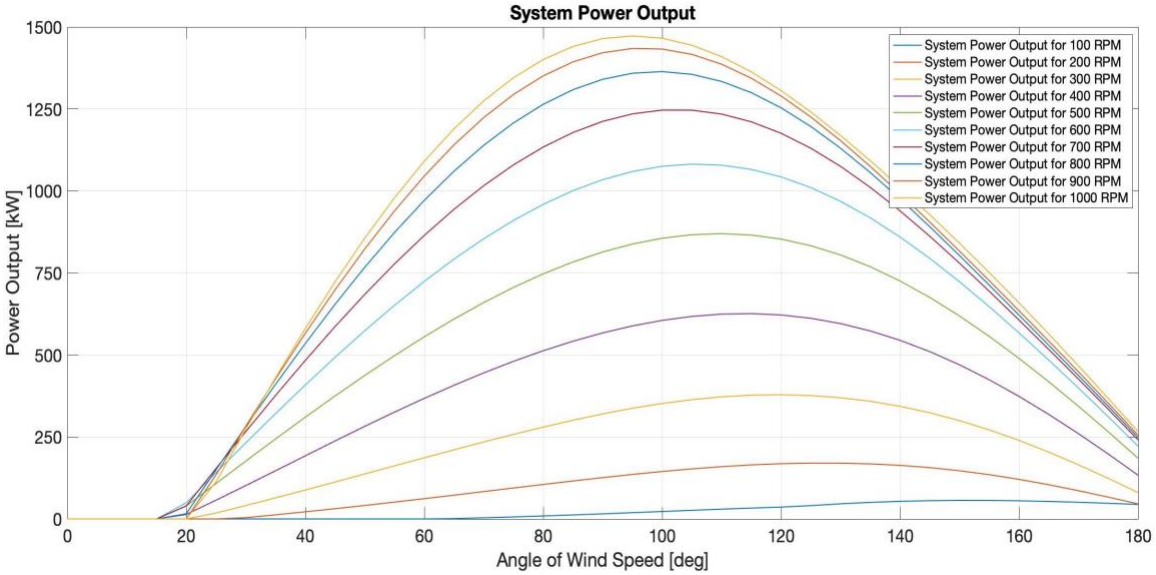

Figure 15: System Power Output

3.7.1.3 Results of the net power output of the system for Flettner rotor speeds from 100 RPM to 1000 RPM

The results have been calculated through the aforementioned model, which utilizes the for-loop function and dynamically plots the 10 different outputs as seen in Figure 16:

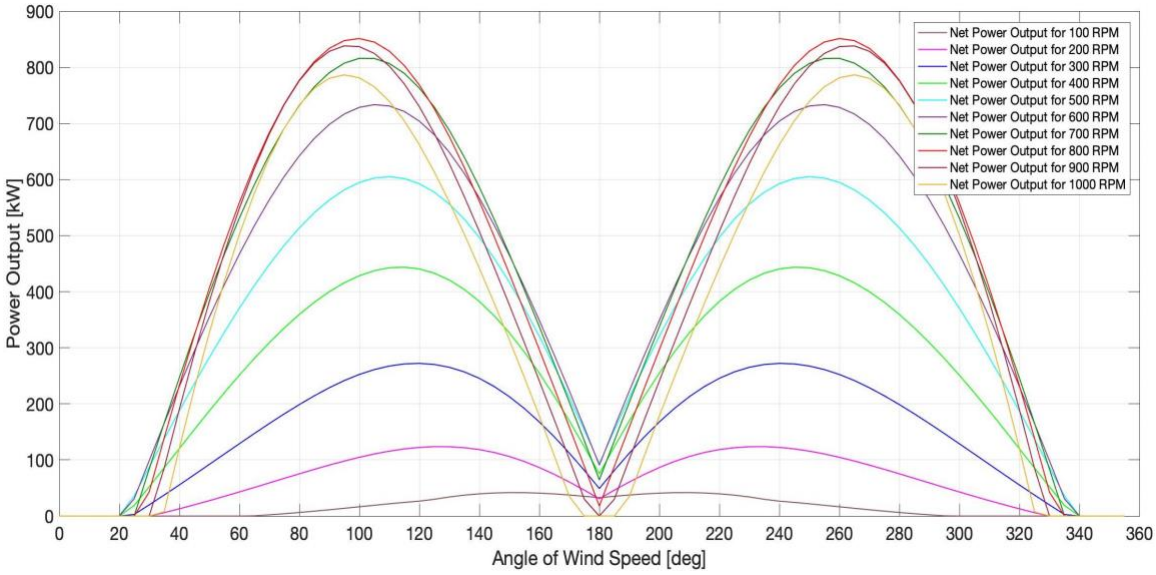

Figure 16: 360º Range of Net Power Output

A symmetry between 0° to 180° and 180° to 360° exists in Figure 16. This result is also logical as the Flettner rotors are capable to rotate clockwise and counterclockwise so the wind affects the vessel the same way whether it comes from the starboard or the port side. So, to present a better image of the net power output, Figure 17 has a range of 0° to 180° since for bigger values the results are repeated.

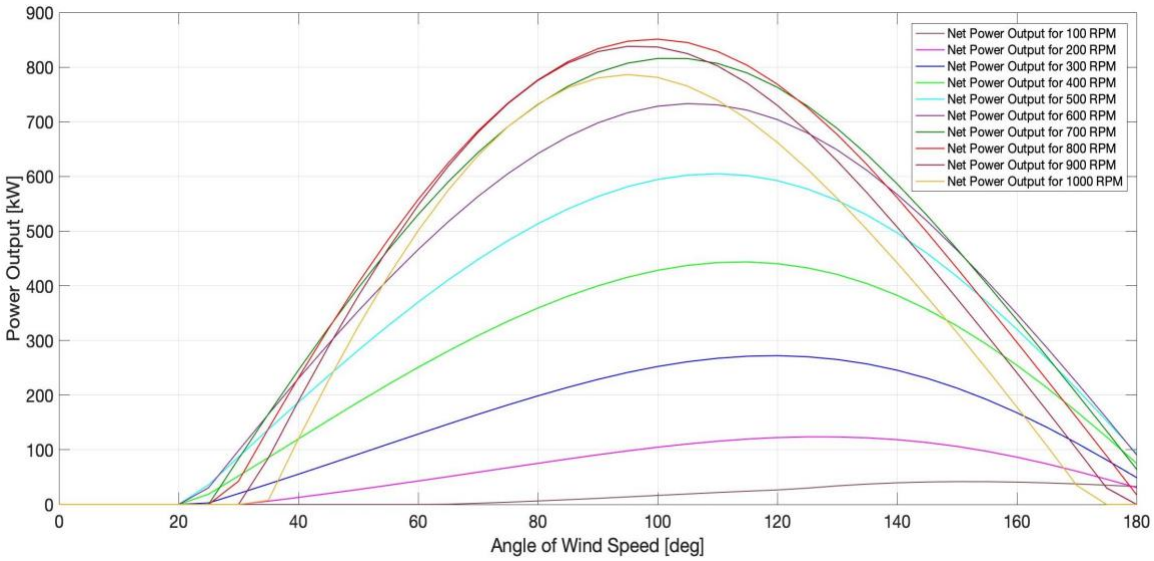

Figure 17: 180º Range of Net Power Output

3.7.1.4 Results of the effective power output of WASP

Having the net power output data, the $F(V_{ref})_{i,j}$, the $W_{i,j,}$ and the $P(V_{ref})_{i,j}$ generated through a series of for-loops from the Matlab code, the effective power output can be calculated. To ensure that the model is well optimized for every possible state of true wind it is important to compare the values between all the rotational speeds of the rotor in order to maximize the power output. After the completion of these procedures, the effective power output of WASP is generated:

$$\left(f_{eff} \cdot P_{eff}\right) = 71.686\ kW \tag{3.21}$$

3.7.2 Results of vessel's EEDI with one Flettner rotor

To generate the results of EEDI is a rather easy procedure at this point as the EEDI (without WASP) is known from chapter 3.2 and the effective power output of the wind propulsion system has been calculated in chapter 3.7.1.4. Thus, the EEDI is calculated through the formula below:

$$EEDI_{new} = EEDI - \frac{f_{eff} \cdot P_{eff} \cdot 3.114 \cdot 170}{15.25 \cdot 89506} = 4.1972\ [\mathrm{g - CO_2/ton - mile}] \tag{3.22}$$

The outputs from chapters 3.7 to 3.7.2 were generated through the help of a more sophisticated Matlab code regarding the implementation of the Global Wind Probability Matrix [25], compared to the code used in chapters 3.3 - 3.6.1. The code developed to model and produce the EEDI index and all the aforementioned results are attached to Appendix II.

3.7.3 Conclusions

For using a single Flettner rotor with a height of 20 meters and a radius of 1.2 meters the results above are considered logical. A noteworthy observation from the development of this model is that there are 4 main variables that can have a significant effect on the effective power output of the system and therefore the EEDI index. These variables are the below:

- Flettner rotor main dimensions
- Lift coefficient
- Drag coefficient
- The global wind probability matrix

It is evident from equation 3.22 that if 4 Flettner rotors with the same dimensions were introduced on the deck of the ship the EEDI index will have a value of EEDI = 4.113 [gr_{CO2}/ton-nm] with a reduction rate of 2.65 % compared to the EEDI index without a Flettner rotor. Lastly, it is important to mention that the global wind probability matrix, which was proposed from IMO Guidelines, is a quite conservative approach to the calculation of the available effective power as it takes into account the average of all wind conditions along the main global shipping routes which are not optimal for a WASP system [25]. Therefore, in the following chapters, we will be calculating a variety of wind conditions in order to have a better understanding of the Flettner rotor's capabilities.

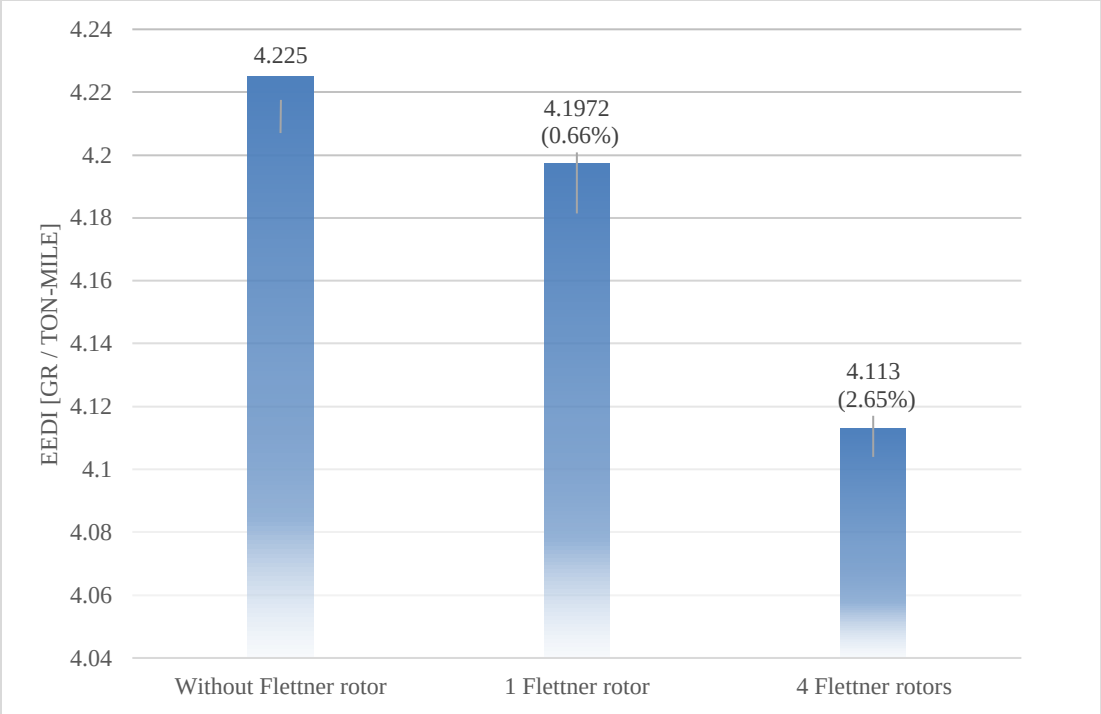

Figure 18: Chart presenting the EEDI indices of different Flettner rotor arrangements

3.8 Results of EEDI index with fixed rotational speed

In the present chapter, we generate the results of the EEDI index for fixed rotational speeds of the rotor. As it is known from chapter 3.7 the EEDI index of the hypothetical system with a 10-gear engine that can move the rotor sail from 100 to 1000 rpm, depending on the wind characteristic, is EEDI=4.1972 [gr_{CO2}/ton-nm] (on optimal rpm). Table 19 is presented a table with 1-gear systems ranging from 100 to 1000 rpm and the reduction rate compared to the EEDI without a Flettner rotor from chapter 3.2.

Table 19: EEDI and Reduction Rate of 1-Rotor Models

Fixed Rotor Speed	EEDI	Increase Rate [%]
100 [RPM]	4.2201	0.55
300 [RPM]	4.2014	0.10
600 [RPM]	4.2086	0.27
800 [RPM]	4.2177	0.49
1000 [RPM]	4.2228	0.61

It is quite noticeable that these systems lose some effective power as they are not as effective as the original 10-gear system, but besides that, the 300 rpm system seems to be the closest to the original system, which is also the industry standard for maximum rotational speeds. It needs to be noted that while the reduction rates may seem quite insignificant, these are 1-rotor models with fixed dimensions and they are utilizing a general global wind probability matrix. The above EEDI indices for fixed rotational speeds were produced from the attached Matlab code in Appendix III.

3.9 Results of EEDI index with specific wind angle and speed

It is important to know the EEDI index in the case of a smaller range of wind angle and speed. In this case the wind angle instead of covering the full 360° now it will be ranging from 80° to 120° and the speed from 1m/s to 14 m/s.

The global wind probability matrix had to also be compromised and normalized to the needs of the study. This was accomplished with the below extra lines of code:

```
WP=WP(17:25,:);

WP=WP(:,1:17);

sumWP=sum(sum(WP));

WP=WP./sumWP;
```

At this point and with some minor modifications the results from the code were generated below:

$$\left(f_{eff} \cdot P_{eff}\right) = 154.22\ kW \quad (3.23)$$

$$EEDI = 4.1652\ [\mathrm{g} - \mathrm{CO}_2/\mathrm{ton} - \mathrm{mile}] \quad (3.24)$$

As we can see the effective power output has more than doubled from 71.686 kW to 154.22 kW and the EEDI index has been reduced significantly. The results of which are developed and produced from the Matlab code attached to Appendix IV.

3.10 EEDI index for constant wind characteristics

In this chapter, two figures are presented, based on the results generated from the Matlab code in Appendix V. These data are corresponding to the EEDI index if the vessel was traveling at a specific speed and with a constant wind speed and angle.

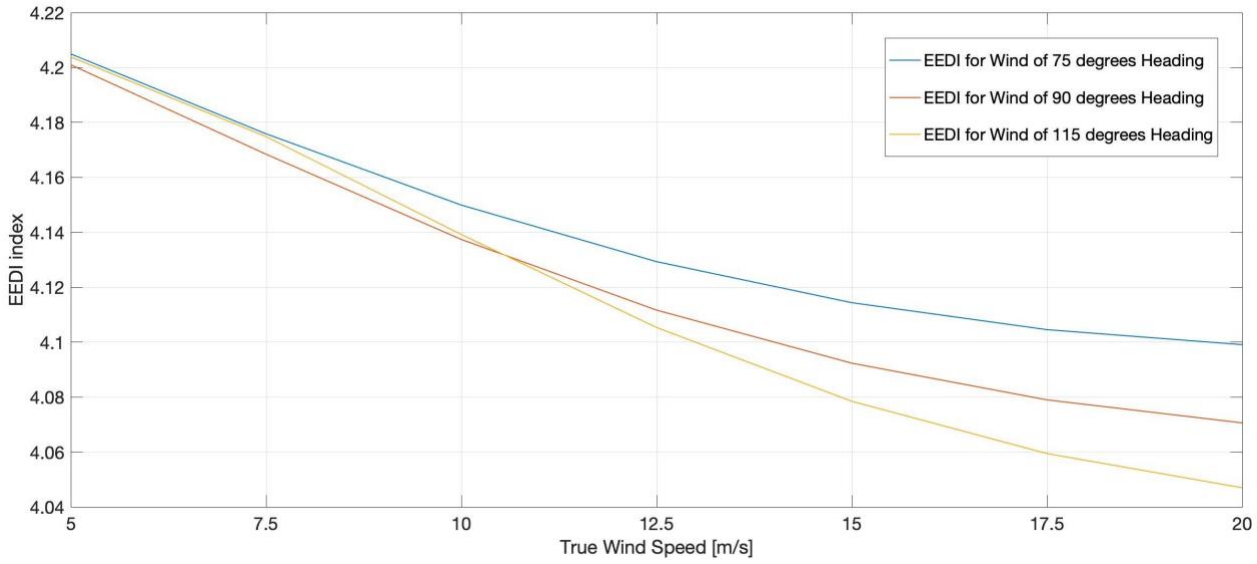

Figure 19: EEDI index of 1-Rotor Model with 100-300 RPM Range

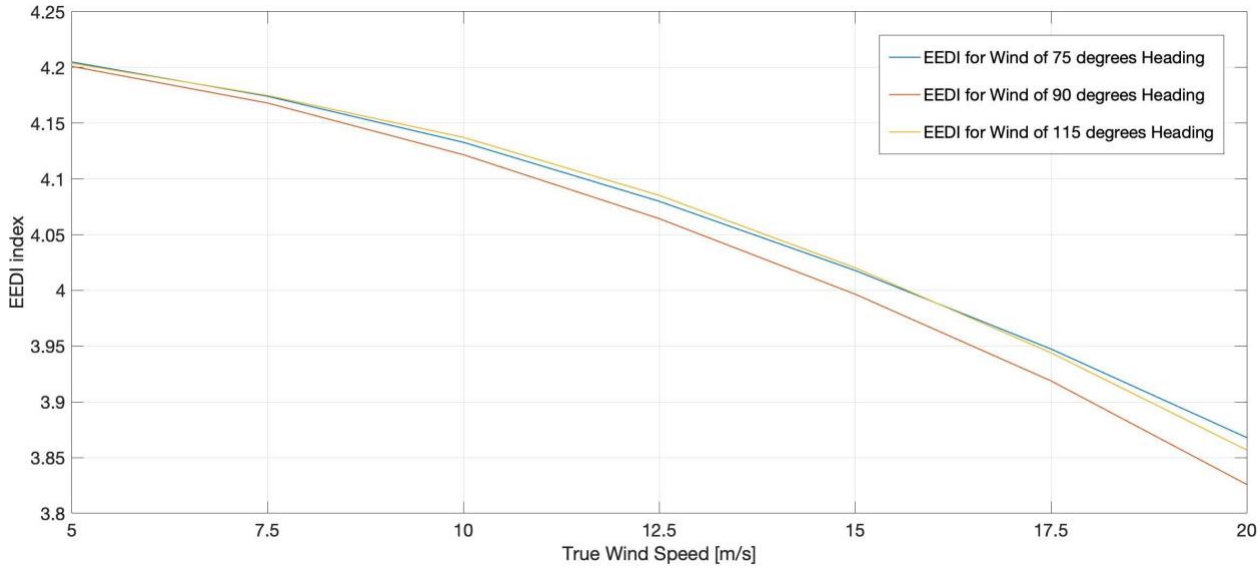

Figure 20: EEDI index of 1-Rotor Model with 100-1000 RPM Range

The difference between these two figures is that the first one is equipped with a 3-gear rotor sail with a speed ranging from 100-300 rpm and the second is equipped with a 10-gear rotor sail with a speed ranging from 100-1000 rpm. The second setup doesn't seem very well commercially known.

3.10.1 Observations

It is important to note that this is a 1-rotor system with dimensions of 20 meters [height] and 1.2 meters [radius]. A more typical configuration, by modifying the code attached to Appendix IV, will be 24 meters [height] by 2 meters [radius]. In that case, the results of chapter 3.9 will be:

$$\left(f_{eff} \cdot P_{eff}\right) = 308.004\ kW = 2.27\% \cdot MCR$$

$$EEDI = 4.1055\ [\mathrm{g} - \mathrm{CO_2}/\mathrm{ton} - \mathrm{mile}], Reduction\ Rate = 2.83\ \%$$

The dimensions of the rotor sails are very important to the final results because, with a 1-rotor system, the vessel is 2.83% more efficient compared to the same vessel without a Flettner rotor.

4 Flettner Rotor – Case Study

In this case study the assessment of the Energy Efficiency Design Index (EEDI) for a bulk carrier will be executed through two distinct methodologies. First, the original method, proposed by the IMO and used in chapter 3, for calculating the EEDI will be implemented on the vessel without any wind-assisted propulsion system. Then the procedure will be repeated for the same vessel equipped with 4 Flettner rotors. Subsequently, another methodology will be utilized related to the IMO document MEPC. 232 (65) [34], which entails a series of calculations to determine the total propeller thrust of the vessel and ultimately the power demand from the engine. The results of the aforementioned procedures will be compared with the intent of identifying some significant conclusions.

4.1 Ship Characteristics

For the purpose of this case study, we will be using a bulk carrier as the vessel of reference. The aforementioned is a ship that we designed during the university course "Marine Vessel Study and Design". The following Table 20 are some of the most basic and important particulars:

Table 20: Ship's Main Particulars

Length between Parallels LBP	225 [m]
Breadth B	36.1 [m]
Design draught T_d	14.35 [m]
Design displacement	87866.8 [tons]
P_{MCR} Main Engine	14644.89 [kW]
Type of fuel (ME)	HFO
Type of fuel (AE)	Diesel Oil

4.2 Calculation of the Velocity

In order to determine the energy efficiency of a ship, it is necessary to estimate the velocity of the ship at its design draft condition while operating at 75% of its rated power. This information was obtained by collecting data from the following diagrams. These are plots of the shaft horsepower (SHP) in PS and Vessel speed in knots versus the rotational speed of the propeller in RPM.

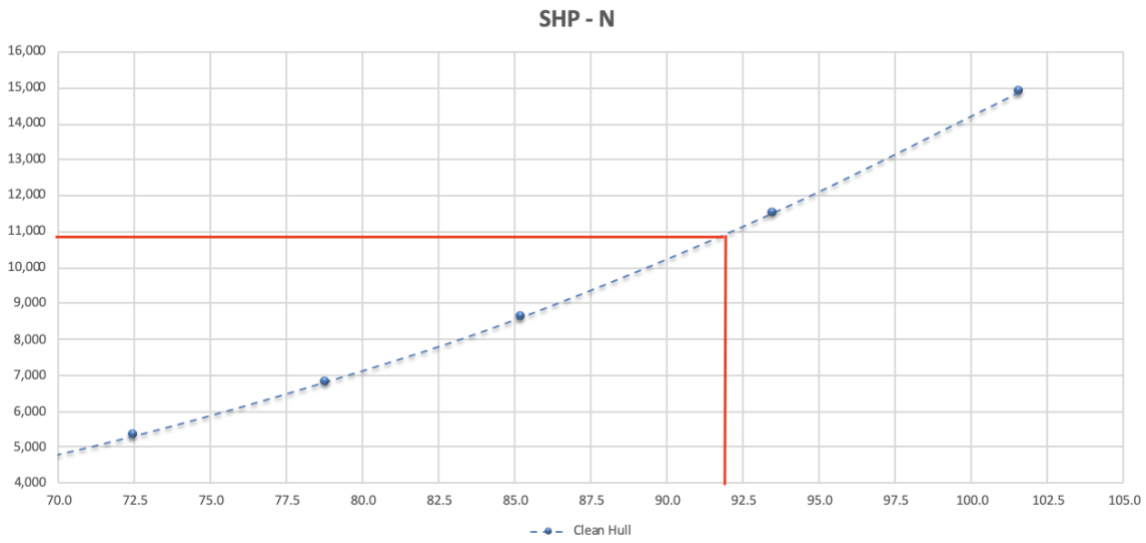

Figure 21: Diagram of SHP (kW) - N (RPM)

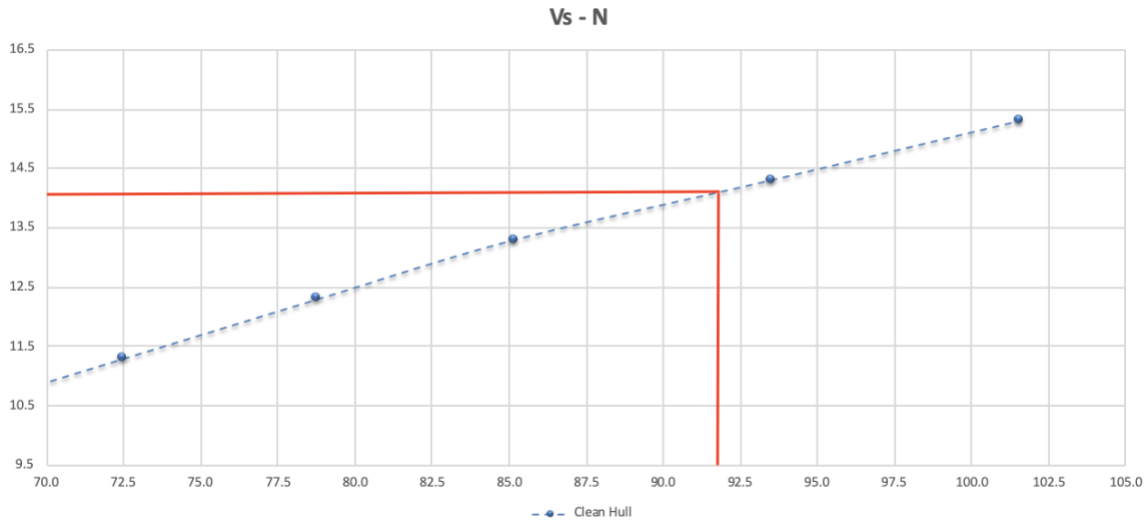

Figure 22: Diagram of Vs (knots) - N (RPM)

Through examination of the aforementioned graphs, we were able to determine the ship's speed in a clean hull condition by first identifying the rotational speed of the propeller at 75% of its rated power from the "SHP-N" graph, and subsequently utilizing the reduction method to calculate the velocity speed from the "Vs-N" graph. The calculated results are presented below:

$$P_{ME} = 75\% \cdot P_{MCR} = 10983.67\ kW = 14933.63\ PS \quad 4.1$$

$$N = 92\ RPM \quad 4.2$$

$$V_S = 14.1\ knots \quad 4.3$$

4.3 EEDI Calculation

4.3.1 EEDI Calculation of Vessel without a Flettner rotor

Emissions from the Main Engine are defined based on a specific power, which is at P_{ME}=0.75*MCR = 10983.67 kW as seen in the previous chapter. That is, one operating point of the Main Engine is considered.

Since the installed power is MCR= 14644.89 kW > 10000 kW, the auxiliary power is calculated based on the relationship: P_{AE} = 0.025*MCR + 250 = 616.12 kW

Specific Fuel Consumption (SFC):

For the main engine, it is calculated at 75% of the load, while for the auxiliary (AE) at 50% of the load. From the Marine Installation Manual of the main engine "WIN GD X62-S2.0" [35] the SFC at 75% is SFC_{ME}= 155.6 gr/kWh as Figure 23 shows:

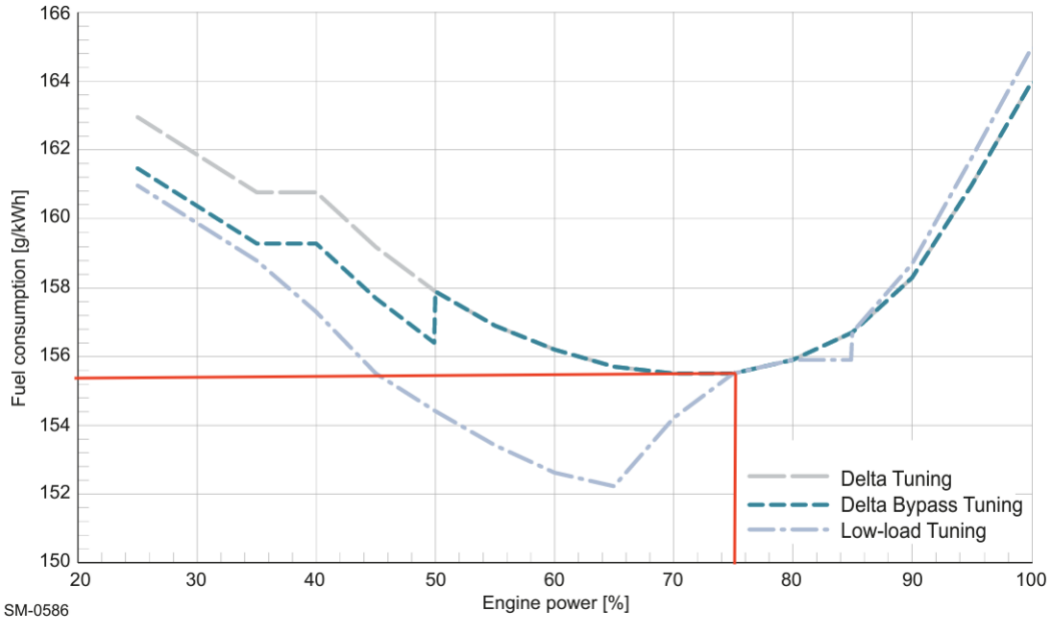

Figure 23: Graph of the Fuel oil consumption of the Main Engine for every load condition [35]

Lastly, from Table 21 it is given that the auxiliary SFC is SFC_{AE}= 202.95 gr/kWh.

The carbon factor for HFO and Diesel Oil fuel is equal to 3.114 t-CO_2/t-Fuel and 3.206 t-CO_2/t-Fuel respectively.

Table 21: Specific Fuel Consumption of Auxiliary Engine on different loads

Load (%)	SFC AE (gr/kWh)
25	214.5
50	202.95
75	187
100	191.95

Ship's speed (V_S):

That velocity has been calculated in the previous chapter thoroughly through the "SHP-N" and "Vs-N" graphs and it is equal to V_S = 14.1 knots.

EEDI Calculation:

From all the data above the achieved EEDI index is calculated as:

$$EEDI = \frac{1*(10983.67*3.114*155.6)+(616.12*3.206*202.95)+0+0}{1*1*87866*1*14.1} = 4.619\ (g - CO_2\ /ton - mile) \quad 4.4$$

4.3.2 EEDI Calculation of a Vessel with a WASP system

In the present case study, it is assumed that the vessel has been equipped with 4 Flettner rotors along the deck. Each cylinder dimension is considered as a radius of R_{fr}=1.2 m and height H=20 m, which are identical to the rotor sail used in previous chapters, thereby allowing for the utilization of the same lift and drag coefficients. Additionally, the rotational speed of the Flettner rotor, ω, is considered to be constant at 500 rpm. The reasoning behind the choice of a steady rotational speed of the rotors is that the primary focus of this case study is to compare EEDI indexes between different calculation methodologies without the influence of extraneous variables.

For the same reason, the wind conditions in this study will be also constant, covering all the main scenarios. Specifically, two true wind angles of 50º (headwind) and 100º (downwind) and two true wind speeds of 7.5 m/s and 15 m/s will be considered.

To calculate the new EEDI index, as shown in the previous chapter, it is necessary to first estimate the available effective power of the wind propulsion system. The available effective power of wind propulsion systems as innovative energy-efficient technology is calculated from the formula 3.20.

By modifying the Matlab code that was previously used to calculate the EEDI for a single rotor system, the available effective power can be derived. The results are presented in Table 22.

Table 22: Results of the available effective Power for the Vessel with WASP

TRUE WIND SPEED M/S	7.5	POWER RATE [%]	15	POWER RATE [%]
TRUE WIND ANGLE DEG				
50	70.42	0.64	1073.14	9.77
100	424.96	3.87	2141.04	19.49

From the results presented in Table 22, two key observations can be made. The first is that there is a notable difference in the performance of the system between the lower wind speed of 7.5 m/s and the higher wind speed of 15 m/s. Despite the fact that the true wind speed is doubled, the effective power at 15 m/s for both wind angles is more than five times greater than the wind speed at 7.5 m/s. The second is that there is an equally noticeable difference in the performance of the system between the headwind of 50º and the downwind of 100º. As a result, the WASP system is able to produce at the most favorable wind condition effective power of 2141.04 kW which covers almost 20% of the Main Engine's power.

To calculate the EEDI is a straightforward process as the EEDI (without WASP) is already known from the previous chapter and the effective power output of the wind propulsion system has been determined in the current chapter. Thus, the EEDI can be computed using the following formula:

$$EEDI_{new} = EEDI - \frac{f_{eff} \cdot P_{eff} \cdot 3.114 \cdot 155.6}{14.1 \cdot 87866.8} \quad 4.5$$

By incorporating the formula above into the Matlab code, we are able to produce the EEDI indexes for every wind condition and present it below, in Table 23:

Table 23: Results of EEDI for Vessel with WASP system

TRUE WIND SPEED M/S	7.5	REDUCTION RATE [%]	15	REDUCTION RATE [%]
TRUE WIND ANGLE DEG				
50	4.591	0.60	4.199	9.09
100	4.453	3.60	3.782	18.13

The conclusions that were previously mentioned regarding the effective power output also apply to the calculation of the EEDI index. Additionally, it is worth noting that the decrease in the EEDI index reaches values as high as 18%, indicating a significant impact of the wind propulsion system on energy efficiency.

4.3.3 EEDI Calculation of a Vessel with a WASP system using the MEPC. 232 (65) methodology

In this chapter, we will use a different method to calculate the EEDI index by following the guidelines outlined in the IMO document MEPC. 232 (65) [34]. This approach takes into account a wider range of factors, including the interaction of the main engine with the propeller and various resistances. This is intended to provide more complete and accurate results by taking a more holistic approach.

Propeller Thrust:

Having already calculated the vessel's speed at 14.1 knots or 7.25 m/s from chapter 4.2 and keeping the same cases for the wind condition from chapter 4.3.2, the propeller thrust can be examined using the following formula:

$$T = \frac{R_{cw}+R_{air}+R_{aw}}{(1-t)} \quad 4.6$$

Where:

- T: Propeller Thrust
- R_{cw}: Hull resistance in calm water
- R_{air}: Aerodynamic resistance
- R_{aw}: Added resistance in waves
- t: Thrust deduction factor

Hull resistance in calm water, R_{cw}:

The resistance of a ship in calm water was calculated by combining the average values from both the B.S.R.A. and Formdata methods and creating a graph of R (resistance) versus V (velocity).

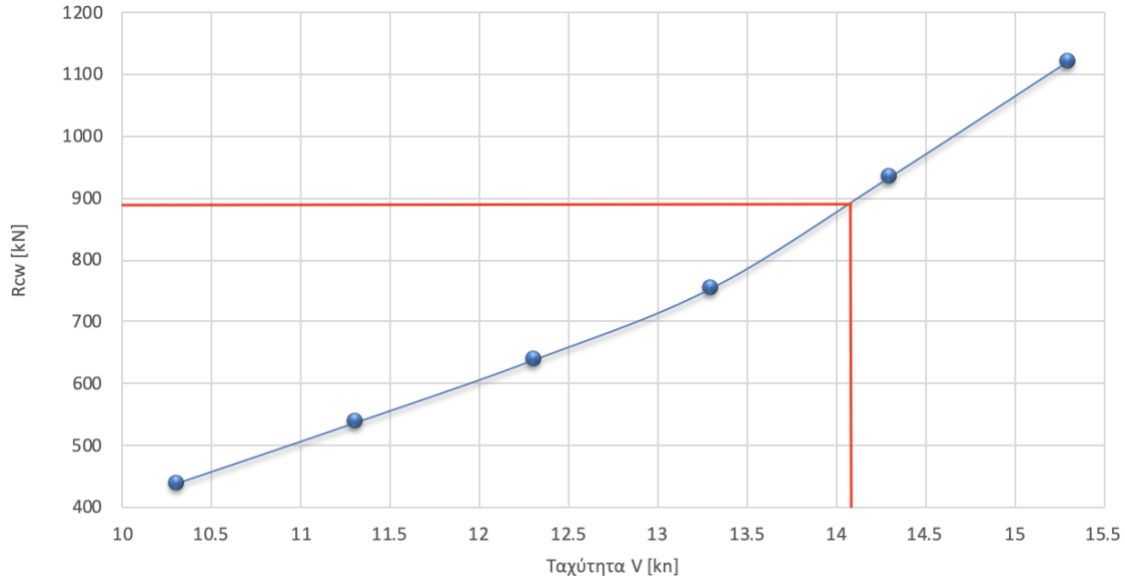

Figure 24: Resistance - velocity graph

The resistance in calm water is shown to have a value of R_{cw} = 892 kN when the ship velocity reaches 14.1 knots, as depicted in the graph of Figure 24.

Aerodynamic resistance, R_{air}:

The aerodynamic resistance can be calculated as:

$$R_{air} = \frac{1}{2} \cdot C_{air} \cdot \rho_a \cdot A_F \cdot V_{w,rel}^2 \quad 4.7$$

Where:

- C_{air} is the aerodynamic resistance coefficient that was obtained by the Sea Trial measurement report of the parent ship. For relative wind direction of 10º – 30º the C_{air} coefficient is ranging from 0.539 to 0.544, which is approximately identical values, and for 90º the C_{air} coefficient has a value of 0.263. With a simple interpolation method, it is possible to generate the value of C_{air} for every apparent wind angle.

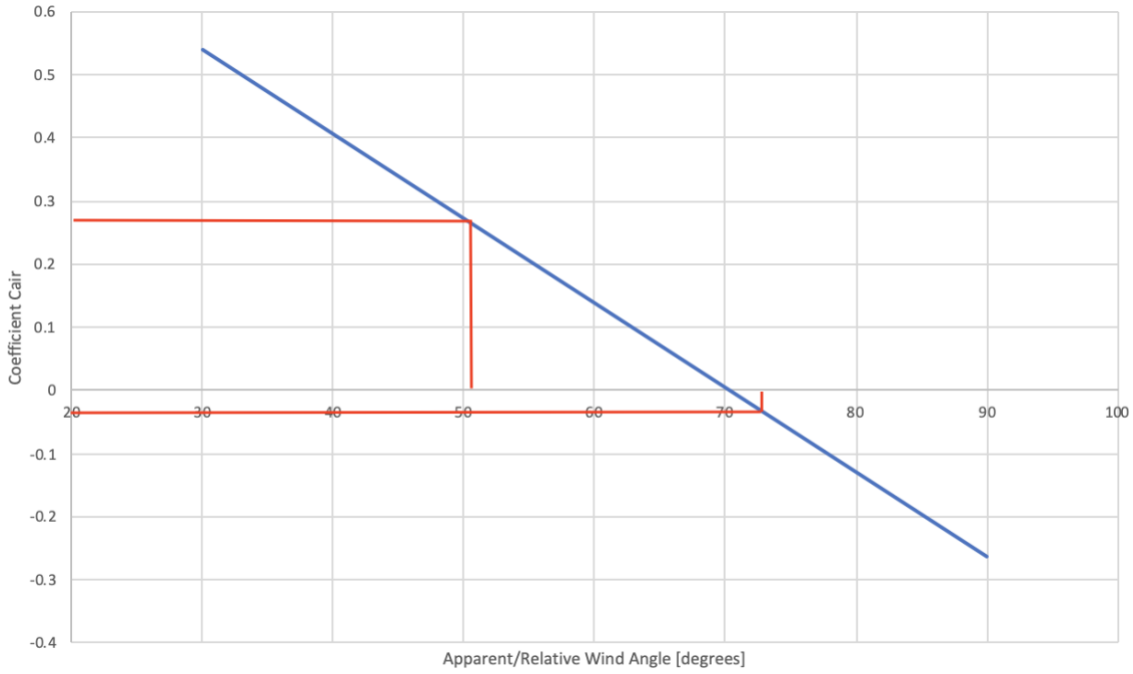

Figure 25: Diagram of aerodynamic resistance coefficient based on data from Sea Trial Measurement report

Table 24: Relative/Apparent wind angle for 4 wind conditions

TRUE WIND SPEED M/S	**7.5**	**CAIR**	**15**	**CAIR**
TRUE WIND ANGLE DEG				
50	25.45	0.544	34.22	0.539
100	51.14	0.285	72.53	-0.04

- ρ_a is the density of air in kg/m^3.
- A_F is the frontal windage area of the hull and superstructure and has the value of A_F = 585.31 m^2.
- $V_{w,rel}$ is the relative wind speed or apparent wind speed in m/s and can be generated through the Matlab code for the four wind conditions that are under examination. Therefore, in Table 25 the results of $V_{w,rel}$ are presented.

Table 25: Relative/Apparent wind speed for 4 wind conditions in m/s

TRUE WIND SPEED M/S	**7.5**	**15**
TRUE WIND ANGLE DEG		
50	13.372	20.433
100	9.485	15.486

The value of aerodynamic resistance, as determined from the data above, is presented in the following Table 26:

Table 26: Results of aerodynamic resistance in N

TRUE WIND SPEED M/S	**7.5**	**15**
TRUE WIND ANGLE DEG		
50	34871.50	80673.49
100	9192.75	-3439.16

Added resistance in waves, R_{aw}:

To calculate the added resistance the STAWAVE 1 method will be used which only includes frontal waves with small width heave and pitch. Due to the small amplitude motions being considered, their effect on the added resistance is considered negligible, so the added drag is solely due to ripple reflection resistance.

At this point of the calculation will only be considered the wind conditions with a true wind angle of 50º as they are the only ones capable of producing frontal waves.

The calculation of the added wave resistance is presented below:

$$R_{AWL} = \frac{1}{16} \cdot \rho \cdot g \cdot h_s^2 \cdot B \cdot \sqrt{\frac{B}{L_{BWL}}} \quad 4.8$$

Where:

- ρ is the seawater density in kg/m^3
- g is gravity acceleration in m/s^2
- h_s is the significant wave height in m. It is important to note that it is not related directly to the wind speed and it varies depending on the specific location and weather conditions, however from a paper published about a numerical prediction of added power in seaway, we managed to correlate the true wind speed to the significant wave height [36]. The results are produced and presented by the following Figure 26 and Table 27:

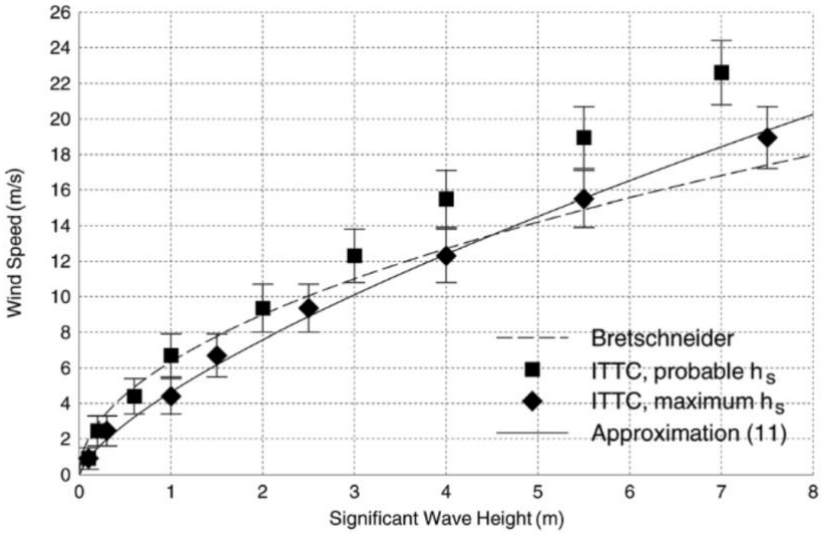

Figure 26: Graph of wind speed - significant wave height, with numerical prediction [36]

Table 27: Results of Significant Wave Height, h_s

True Wind Speed (m/s)	Significant Wave Height (m)
7.5	1.5
15	4.5

- B is the Breadth of the vessel in m
- L_{BWL} is the length of the bow section in the water line which corresponds to 95% of the ship's width

The following Table 28 shows the calculated value of added resistance in waves, R_{aw}, based on the data analyzed.

Table 28: Results of added resistance in waves, R_{aw} in N

TRUE WIND SPEED M/S	**7.5**	**15**
TRUE WIND ANGLE DEG		
50	48800.08	439200.69

Delivered power to the propeller, P_D:

Having calculated all the individual resistances, the total resistance R is:

$$R = R_{cw} + R_{air} + R_{aw} \quad (4.9)$$

Thus, the thrust T of the propeller is calculated as:

$$T = \frac{R}{1-t} \quad (4.10)$$

Where the thrust deduction factor t was obtained through the average of the following empirical formulas: SSPA, Hecksher, and Danckwardt. The wake fraction (w) can also be obtained through model tests or an empirical formula, with default conservative estimates provided in the following table:

Table 2: Recommended values for wake fraction *w*

Block coefficient	One propeller	Two propellers
0.5	0.14	0.15
0.6	0.23	0.17
0.7	0.29	0.19
0.8 and above	0.35	0.23

For the current case study w=0.42 and t=0.245. Thus, it is able to calculate the thrust of the propeller in kN for every wind condition. By deducting the effective force F_x from the required thrust of the propeller the WASP system is incorporated into the calculation of the delivered power to the propeller and ultimately to the EEDI index:

Table 29: Thrust of the propeller based on the resistances applied to the vessel and the deducted thrust in kN

TRUE WIND SPEED M/S	**7.5**		**15**	
TRUE WIND ANGLE DEG	T	$T_{deducted}$	T	$T_{deducted}$
50	1292.28	1260.14	1870.03	1734.22
100	1193.63	1124.84	1176.90	930.67

After producing results from a series of formulas, which are presented below, we calculate the delivered power to the propeller P_D and therefore the BHP of the vessel by incorporating the n_t transmission coefficient.

$$V_a = V_s \cdot (1 - w) \quad 4.11$$

$$\frac{K_T(J)}{J^2} = \frac{T}{\rho \cdot V_a^2 \cdot D_P^2} \quad 4.12$$

$$n = \frac{V_a}{J \cdot D_P} \quad 4.13$$

$$P_D = 2\pi \cdot \rho \cdot n^3 \cdot D_P^5 \cdot K_Q(J)/n_R \quad 4.14$$

$$BHP = \frac{P_D}{n_t} \quad 4.15$$

Table 30: Brake horsepower of the vessel in kW

TRUE WIND SPEED M/S	**7.5**		**15**	
TRUE WIND ANGLE DEG	BHP [kW]	N [RPM]	BHP [kW]	N [RPM]
50	12130.89	96.8	18136.24	108.4
100	10527.55	92.5	8310.14	84.3

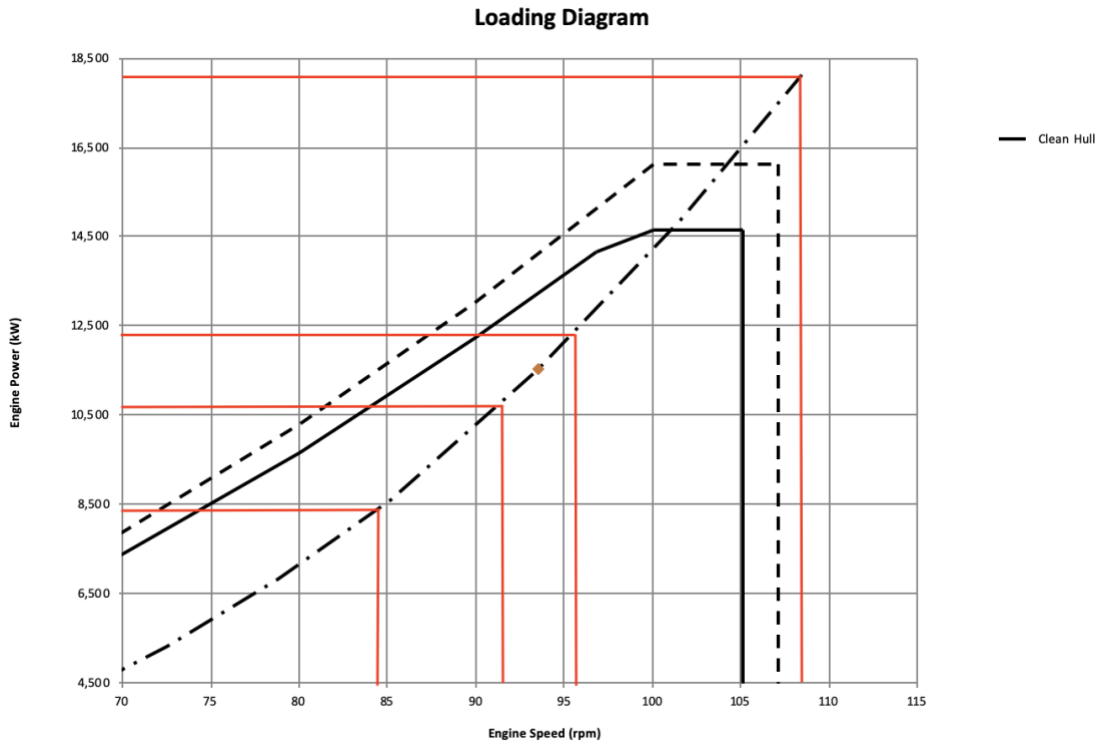

Figure 27: Main Engine Loading Diagram

To conclude, the results of the EEDI index for all four wind conditions were calculated using the methodology outlined in the IMO document MEPC.232(65) [34]. This method considers not only the interactions between the vessel and weather conditions but also the mechanical capabilities of the propeller, providing a more comprehensive and in-depth approach to EEDI calculations than the IMO's proposed method [23].

The following Table 31 displays the results of the EEDI index for each wind condition and the reduction rate compared to the EEDI calculated in chapter 4.3.2.

Table 31: Results of EEDI for Vessel with WASP system using MEPC. 232 (65)

TRUE WIND SPEED M/S	**7.5**	**REDUCTION RATE [%]**	**15**	**REDUCTION RATE [%]**
TRUE WIND ANGLE DEG				
50	5.068	-10.39	7.417	-76.63
100	4.441	0.27	3.574	5.51

When the wind conditions are intensifying, the results of Table 31 are showcasing a significant discrepancy compared to those of Table 23. This is a logical conclusion as it is known that with the method from chapter 4.3.2, the added resistances of the vessel are not considered. Therefore, in Figure 28, the differences between the two methods are visualized.

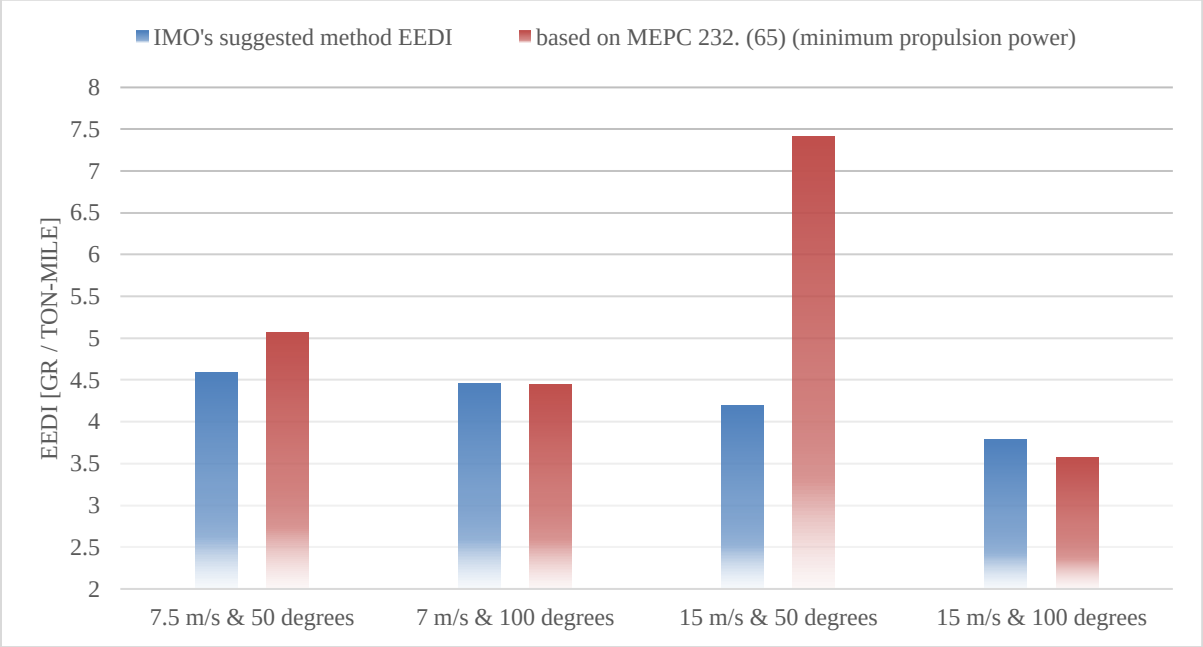

Figure 28: Chart comparing the 2 methods of the Case Study

5 Conclusions

The current study amasses a substantial quantity of data regarding the energy efficiency of Flettner rotors, which are highly considered as one of the preeminent Wind-Assisted Propulsion Systems (WASP). To begin with, the principle of operation of the Flettner rotor was described. Subsequently, a series of Matlab codes were developed and employed to generate various results relating to the energy aspect of the rotor, with the ultimate goal of determining the Energy Efficiency Design Index (EEDI). The study presents and compares the EEDI results under various wind conditions, as well as for rotors with diverse mechanical properties, thereby providing a deeper understanding of the energy capabilities of Flettner rotors.

The findings from chapter 3 indicate that the results of the power propulsion of the rotor are significantly influenced by its dimensions, mechanical and structural properties, as well as the wind conditions encountered by the vessel.

Upon comparing a 10-gear rotor system with rotational speeds ranging from 100 to 1000 rpm to a rotor sail with a fixed rotational speed and utilizing the Global Wind Probability Matrix to calculate the EEDI, it was observed that the results are comparable, with the 10-gear rotor sail exhibiting a mere 0.1% greater efficiency than the rotor sail with a constant rotational speed of 300 rpm. Although it should be noted that the increase rate of the rotor's efficiency would be much higher if more specific wind conditions rather than the Global Wind Probability Matrix were considered.

However, when the vessel encounters consistent wind angles within the operational range of the Flettner rotor, the number of gears the rotor possesses significantly affects its efficiency. As presented in chapter 3.10 the results of the EEDI index of two different Wind-assisted Propulsion Systems (WASP) are depicted in Figure 19 and Figure 20. The 10-gear WASP system was found to be significantly more efficient than the 3-gear WASP system, with the EEDI reaching a minimum value of 3.83 [gr_{CO2}/ton-nm] under optimal conditions, compared to 4.05 [gr_{CO2}/ton-nm] for the latter system.

In chapter 3.10.1, another crucial comparison was made, relating to the dimensions of the rotor. The integration of a slightly larger Flettner rotor in terms of height and width was observed to result in a further reduction of the EEDI index by 1.43%, a substantial reduction rate given the narrow power margin of a WASP system. It should also be noted that this result should be considered an approximation rather than an exact determination, as the aerodynamic coefficients of rotor sails vary based on their dimensions.

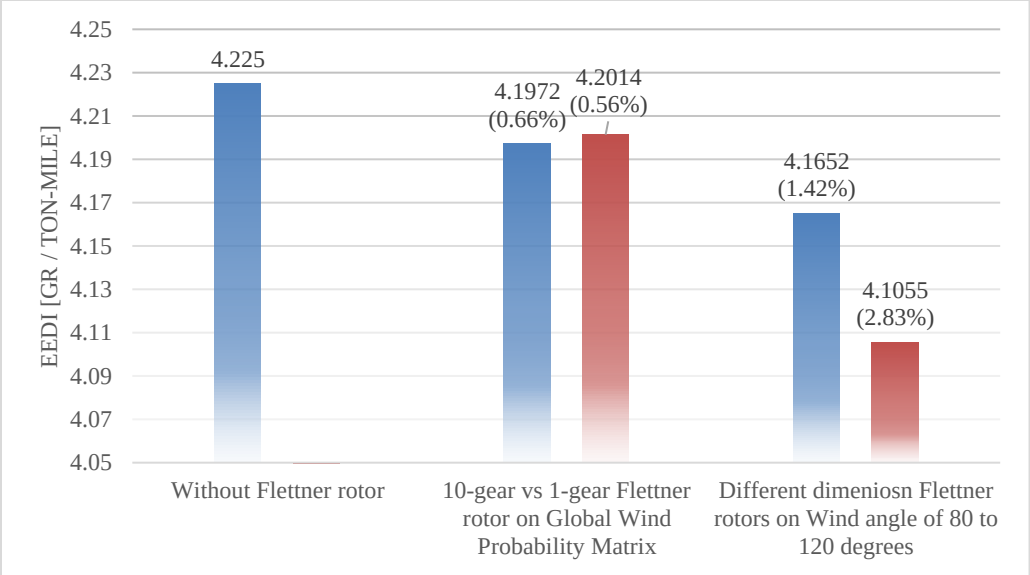

Figure 29: Chart comparing results between different Flettner rotor arrangements from chapter 3

Furthermore, a case study was performed to evaluate the Energy Efficiency Design Index (EEDI) through two distinct methodologies. Initially, the original method of calculating EEDI was employed, and then the MEPC.232 (65) methodology was utilized. In comparison to the conventional EEDI calculation process, which is recommended by the International Maritime Organization (IMO), the latter methodology necessitates a series of calculations to determine the total propeller thrust of the vessel and ultimately calculate the power required from the engine.

The results of this case study highlight the significance of wind conditions and their impact, not only on the Flettner rotor but on the vessel as a whole. It is crucial to take into account the forces exerted by wind and waves, as they can significantly impact the results and energy efficiency of the vessel if not properly considered. According to the proposed approach by the International Maritime Organization (IMO), the computation of the Flettner rotors' effective power output does not incorporate wind and wave resistances. This is in contrast to the methodology described in the MEPC.232 (65), which takes these resistances into account. The power efficiency of Flettner rotors is significantly affected by the direction and velocity of the wind, and can be diminished when the wind opposes the ship's motion, but also increased when the wind is in favor of the ship's motion.

There is still much to be discovered about innovative technologies such as Flettner rotors, and further investigation is necessary to f. In the current study, we have not factored in the lateral forces and yaw moments, which are crucial to the efficiency assessment of all types of sails. Additionally, it is essential to consider the structural and operational limitations of Flettner rotors, as their structural integrity and safety are preeminent concerns. Moreover, aerodynamic interactions between two or more Flettner rotors

should not be disregarded; on the contrary, it is an intriguing field where innovative solutions to minimize drag are constantly being proposed.

References

[1] "Fourth Greenhouse Gas Study 2020." https://www.imo.org/en/OurWork/Environment/Pages/Fourth-IMO-Greenhouse-Gas-Study-2020.aspx (accessed Feb. 01, 2023).

[2] M. Bentin, D. Zastrau, M. Schlaak, D. Freye, R. Elsner, and S. Kotzur, "A New Routing Optimization Tool-influence of Wind and Waves on Fuel Consumption of Ships with and without Wind Assisted Ship Propulsion Systems," in *Transportation Research Procedia*, 2016, vol. 14, pp. 153–162. doi: 10.1016/j.trpro.2016.05.051.

[3] J. C. Mason, J. Broderick, and A. Larkin, "Quantifying voyage optimisation with wind-assisted ship propulsion: a new climate mitigation strategy for shipping."

[4] A. Flettner, "Die Anwendung der Erkenntnisse der Aerodynamik zum Windantrieb von Schiffen," in *Jahrbuch der Schiffbautechnischen Gesellschaft: Fünfundzwanzigster Band*, Berlin, Heidelberg: Springer Berlin Heidelberg, 1925, pp. 222–251. doi: 10.1007/978-3-642-92026-4_11.

[5] "Rotor Sail Technology - Anemoi Marine." https://anemoimarine.com/rotor-sail-technology/ (accessed Feb. 01, 2023).

[6] "Rotor Sail Technology | Norsepower." https://www.norsepower.com/technology/ (accessed Feb. 01, 2023).

[7] C. Hcini, E. Abidi, B. Kamoun, and D. Afungchui, "Numerical prediction for the aerodynamic performance of Turbosail type wind turbine using a vortex model," *Energy*, vol. 109, pp. 287–293, Aug. 2016, doi: 10.1016/J.ENERGY.2016.04.113.

[8] G. Bordogna, J. A. Keuning, R. H. M. Huijsmans, and M. Belloli, "Wind-tunnel experiments on the aerodynamic interaction between two rigid sails used for wind-assisted propulsion," *International Shipbuilding Progress*, vol. 65, no. 1, pp. 93–125, Jan. 2018, doi: 10.3233/ISP-180143.

[9] "Norsepower Rotor Sails confirmed savings of 8.2 % fuel and associated CO2 in Maersk Pelican project — Maersk Tankers." https://maersktankers.com/newsroom/norsepower-rotor-sails-confirmed-savings (accessed Feb. 01, 2023).

[10] "Berge Bulk Adds Rotor Sails to Two Giant Bulkers." https://maritime-executive.com/article/berge-bulk-adds-rotor-sails-to-two-giant-bulkers (accessed Feb. 01, 2023).

[11] "Newbuild Vale VLOC Revealed as Bulk Carrier Getting Five Tilting Rotor Sails." https://gcaptain.com/newbuild-vale-vloc-revealed-as-bulk-carrier-getting-five-tilting-rotor-sails/ (accessed Feb. 01, 2023).

[12] "MV Afros 21st Century Technology | Blue Planet Shipping LTD." https://www.blueplanetshipping.gr/news/mv-afros-21st-century-technology/ (accessed Feb. 01, 2023).

[13] N. Vasileiadis, "Dynamic Analysis of Hydrofoils and Flettner Rotors Implemented on a Marine Cloud Brightening Spray Vessel," 2022. Accessed: Feb. 01, 2023. [Online]. Available: https://www.cemt.eu/PostGradMarTec2022.html

[14] S. Salter, G. Sortino, and J. Latham, "Sea-going hardware for the cloud albedo method of reversing global warming," *Philosophical Transactions of the Royal Society A: Mathematical, Physical and Engineering Sciences*, vol. 366, no. 1882, pp. 3989–4006, Nov. 2008, doi: 10.1098/RSTA.2008.0136.

[15] J. Latham, B. Parkes, A. Gadian, and S. Salter, "Weakening of hurricanes via marine cloud brightening (MCB)," *Atmospheric Science Letters*, vol. 13, no. 4, pp. 231–237, Oct. 2012, doi: 10.1002/ASL.402.

[16] L. Prandtl and A. Betz, *Ergebnisse der Aerodynamischen Versuchsanstalt zu Göttingen, 4th version. Berlin and Munich*, 4th ed. 1932.

[17] Martina Reche-Vilanova, "Performance Prediction Program for Wind-Assisted Cargo Ships." Accessed: Feb. 01, 2023. [Online]. Available: https://www.researchgate.net/publication/344238090_Performance_Prediction_Program_for_Wind-Assisted_Cargo_Ships

[18] G. Bordogna, "Aerodynamics of wind-assisted ships Interaction effects on the aerodynamic performance of multiple wind-propulsion systems," 2020, doi: 10.4233/uuid:96eda9cd-3163-4c6b-9b9f-e9fa329df071.

[19] "Energy Efficiency Measures." https://www.imo.org/en/ourwork/environment/pages/technical-and-operational-measures.aspx (accessed Feb. 01, 2023).

[20] "2013 GUIDANCE ON TREATMENT OF INNOVATIVE ENERGY EFFICIENCY TECHNOLOGIES FOR CALCULATION AND VERIFICATION OF THE ATTAINED EEDI," 2013.

[21] M. Polakis, P. Zachariadis, and J. O. de Kat, "The energy efficiency design index (Eedi)," *Sustainable Shipping: A Cross-Disciplinary View*, pp. 93–115, Jan. 2019, doi: 10.1007/978-3-030-04330-8_3/FIGURES/13.

[22] IMO, “Module 2: Ship Energy Efficiency Regulations and Related Guidelines.”

[23] “MEPC.1-Circ.896”.

[24] “MEPC 74/INF.39 - Findings on the EEDI assessment framework for wind propulsion systems.”

[25] “MEPC 62/INF.34, REDUCTION OF GHG EMISSIONS FROM SHIPS Global Wind Specification along the Main Global Shipping Routes to be applied in the EEDI Calculation of Wind Propulsion Systems,” 2011.

[26] “MEPC 79-INF.21 - Wind Propulsion (Comoros, Finland, France,...)”.

[27] “Wind triangle – Navalapp.” https://navalapp.com/articles/wind-triangle/ (accessed Feb. 02, 2023).

[28] “Magnus effect - Wikiwand.” https://www.wikiwand.com/en/Magnus_effect (accessed Feb. 02, 2023).

[29] “E-Ship 1 - Wikipedia.” https://en.wikipedia.org/wiki/E-Ship_1 (accessed Feb. 02, 2023).

[30] “ANNEX 5 MEPC.308(73) (adopted on 26 October 2018) Guidelines on the method of calculation of the attained energy efficiency design index (EEDI) for new ships, p. 8.”

[31] “Sail Shape Optimization with CFD, fig. 6.” Accessed: Feb. 02, 2023. [Online]. Available: https://www.researchgate.net/publication/257143505_Sail_Shape_Optimization_with_CFD

[32] D. R. Pearson, “The use of flettner rotors in efficient ship design,” in *Proceedings of the Influence of EEDI on Ship Design Conference*, 2014.

[33] G. S. Lloyd, “Rules for Classification and Construction VI Additional Rules and Guidelines 13 Energy Efficiency 1 Guidelines for Determination of the Energy Efficiency Design Index, p. D-4,” 2013. [Online]. Available: www.gl-group.com

[34] International Maritime Organization, “2013 Interim guidelines for determining minimum propulsion power to maintain the manoeuvrability of ships in adverse conditions.”

[35] “MIM_WinGD_X62-S2.0., fig. 1-4,” 2022.

[36] V. Shigunov, “Numerical prediction of added power in seaway,” *Journal of Offshore Mechanics and Arctic Engineering*, vol. 140, no. 5, Oct. 2018, doi: 10.1115/1.4039955.

Appendix I

```
clear all
close all

% Rotor dimensions
Rfr=1.2;            % Radius in [meters]
Hfr=20;             % Height in [meters]
Afr=2.*Rfr.*Hfr;    % Area of the affected cross-sectional surface in
                      [meters^2]
Ar=2.*pi.*Rfr.*Hfr; % Surface area of the rotor in [meters^2]
rpm=500;            % Rotational speed of the rotor in [rpm]
rs=2.*pi.*rpm./60;  % rpm to rotations per second

%Extra constants
p=1.225;            % Air density in [kg/m^3]
ma=0.0000181;       % Air's dynamic viscosity in [kg/(m*s)]

%Ship Characteristics
Vref=7.8436;        % Ship's reference speed in [m/s]
ht=0.75;            % System's efficiency

%Lift/Drag Coefficients
% Velocity ratio
X=[0,0.5,1,1.5,2,2.5,3,3.5,4,4.5,5,5.5,6,6.5,7,7.5,8];
% Lift Coefficient
Cl=[0,0.2,1,2.5,4.2,6.15,8,9.3,10,10.3,10.9,11,11.1,11.4,11.6,11.7,11.8
];
% Drag Coefficient
Cd=[1,0.8,0.6,0.7,0.9,1.5,2,2.8,3,3.2,3.5,3.6,3.8,3.9,3.95,4,4.1];

Wind_angle=0:45:315;    % True wind angle in [degrees]
Wind_speed=1:5:25;      % True wind speed in [m/s]

% Introduce apparent wind speed & angle matrices
Pv=[];
Pa=[];

% for-loop for apparent wind speed & angle using external function
for i=1:1:length(Wind_angle)
    [V,A]=App_Wind_Speed_Angle(Wind_speed,Vref,Wind_angle(1,i));
    Pv=[Pv;V];
    Pa=[Pa;A];
end
Pa=real(Pa);                % Keeps only the real part of the matrix

Vrat=(rs.*Rfr)./Pv;         % Velocity ratio
Vrat=min(Vrat,8);           % Bounding the value due to the asymptotic
                              form of the lift and drag coefficient
Vrot=rs.*Rfr;               % Linear velocity on the rotor's surface in
                              [m/s]
Re=p.*rs.*Rfr.^2.*(1./ma);  % Reynold's number
Cf=0.0576./(Re.^(1./5));    % Skin friction coefficient
```

```
Ff=0.5.*Cf.*p.*Vrot.^2.*Ar; % Frictional force in [N]
Pcon=Ff.*Vrot;              % Power required to rotate the rotor in
                              [Watts]

% Form of the lift & drag coefficient functions
Clfun=-0.0008259.*Vrat.^6+0.01494.*Vrat.^5-0.05744.*Vrat.^4-
0.3346.*Vrat.^3+2.405.*Vrat.^2-1.075.*Vrat+0.05456;
Cdfun=-0.0007167.*Vrat.^6+0.01705.*Vrat.^5-
0.1437.*Vrat.^4+0.4656.*Vrat.^3-0.2084.*Vrat.^2-0.5551.*Vrat+1.025;

Fl=0.5.*p.*Pv.^2.*Afr.*Clfun;       % Lift force function in [N]
Fd=0.5.*p.*Pv.^2.*Afr.*Cdfun;       % Drag force function in [N]

% Effective force functions in [N]
Fx=Fl.*sin(deg2rad(Pa))-Fd.*cos(deg2rad(Pa));
Fx(imag(Fx)~=0)=0;
Fxcorr=max(Fx,0);
Fy=Fl.*cos(deg2rad(Pa))+Fd.*sin(deg2rad(Pa));

% System power output in [Watts]
Ps=Fxcorr.*Vref;
Pnet=(Ps-Pcon).*ht;
Pnetcorr=max(Pnet,0);
```

Appendix II

```
clear all
close all

% Rotor dimensions
Rfr=1.2;            % Radius in [meters]
Hfr=20;             % Height in [meters]
Afr=2.*Rfr.*Hfr;    % Area of the affected cross-sectional surface in
                      [meters^2]
Ar=2.*pi.*Rfr.*Hfr; % Surface area of the rotor in [meters^2]
rpm=[100:100:1000]; % Rotational speed of the rotor in [rpm]
rs=2.*pi.*rpm./60;  % rpm to rotations per second

% Extra constants
p=1.225;            % Air density in [kg/m^3]
ma=0.0000181;       % Air's dynamic viscosity in [kg/(m*s)]

% Ship Characteristics
Vref=7.8446;        % Ship's reference speed in [m/s]
ht=0.75;            % System's efficiency

%Lift/Drag Coefficients
% Velocity ratio
X=[0,0.5,1,1.5,2,2.5,3,3.5,4,4.5,5,5.5,6,6.5,7,7.5,8];
% Lift Coefficient
Cl=[0,0.2,1,2.5,4.2,6.15,8,9.3,10,10.3,10.9,11,11.1,11.4,11.6,11.7,11.8
];
% Drag Coefficient
Cd=[1,0.8,0.6,0.7,0.9,1.5,2,2.8,3,3.2,3.5,3.6,3.8,3.9,3.95,4,4.1];


Wind_angle=0:5:355; % True wind angle in [degrees]
Wind_speed=1:1:25;  % True wind speed in [m/s]

% Introduce apparent wind speed & angle matrices
Pv=[];
Pa=[];

% for-loop for apparent wind speed & angle
for i=1:1:length(Wind_angle)
    [V,A]=App_Wind_Speed_Angle(Wind_speed,Vref,Wind_angle(1,i));
    Pv=[Pv;V];
    Pa=[Pa;A];
end

Pa=real(Pa);                    % Keeps only the real part of the
                                  matrix

Vrot=rs.*Rfr;                   % Linear velocity on the rotor's
                                  surface in [m/s]
Re=p.*rs.*Rfr.^2.*(1./ma);      % Reynold's number
Cf=0.0576./(Re.^(1./5));        % Skin friction coefficient
```

```
Ff=0.5.*Cf.*p.*Vrot.^2.*Ar;      % Frictional force in [N]
Pcon=Ff.*Vrot;                   % Power required to rotate the rotor in
                                   [Watts]

GW=load('matlab.mat');           % Load global wind probability matrix
WP=cell2mat(struct2cell(GW));    % Transition from cell to matrix

% Introduce cells with dimensions: length(rpm) by 1
Vrat=cell(length(rpm),1);        % Velocity ratio
Fl=cell(length(rpm),1);          % Lift force in [N]
Fd=cell(length(rpm),1);          % Drag force in [N]
Fx=cell(length(rpm),1);          % Effective force parallel to ship's
                                   direction in [N]
Fy=cell(length(rpm),1);          % Effective force vertically to ship's
                                   direction in [N]
Ps=cell(length(rpm),1);          % System power output in [Watts]
PW=cell(length(rpm),1);          % Power consumption * global wind
                                   probability in [Watts]
Clfun=cell(length(rpm),1);       % Lift coefficient function
Cdfun=cell(length(rpm),1);       % Drag coefficient function
Pnet=cell(length(rpm),1);        % Net power output in [Watts]

% for-loop generating data for the above cells (lines 50-60)
for k=1:1:length(rpm)

      Vrat{k}=(rs(k).*Rfr)./Pv;
      Vrat{k}=min(Vrat{k},7.61);      % Bounding the value due to the
                                        asymptotic form of the lift and
                                        drag coefficient

      % form of the lift & drag coefficient functions
      Clfun{k}=-0.0008259.*Vrat{k}.^6+0.01494.*Vrat{k}.^5-
      0.05744.*Vrat{k}.^4-0.3346.*Vrat{k}.^3+2.405.*Vrat{k}.^2-
      1.075.*Vrat{k}+0.05456;
      Cdfun{k}=-0.0007167.*Vrat{k}.^6+0.01705.*Vrat{k}.^5-
      0.1437.*Vrat{k}.^4+0.4656.*Vrat{k}.^3-0.2084.*Vrat{k}.^2-
      0.5551.*Vrat{k}+1.025;

      Fl{k}=0.5.*p.*Pv.^2.*Afr.*Clfun{k}; % Lift force function in [N]
      Fd{k}=0.5.*p.*Pv.^2.*Afr.*Cdfun{k}; % Drag force function in [N]

      % Effective force functions in [N]
      Fx{k}=Fl{k}.*sin(deg2rad(Pa))-Fd{k}.*cos(deg2rad(Pa));
      Fx{k}=real(Fx{k});
      Fx{k}=max(Fx{k},0);
      Fy{k}=Fl{k}.*cos(deg2rad(Pa))+Fd{k}.*sin(deg2rad(Pa));

      % System power output in [Watts]
      Ps{k}=Fx{k}.*Vref;
      Pnet{k}=(Ps{k}-Pcon(k)).*ht;
      Pnet{k}=max(Pnet{k},0);
      PW{k}=WP.*Pcon(k);
end
```

```
% Maximum system power output from 100 to 1000 rpm in [Watts]
Psfinal=cell(length(rpm),1);
for l=1:length(rpm)
      Psfinal{l}=max(Ps{l},[],2);
      PsfinalkW{l}=Psfinal{l}./1000;
end

% Maximum net power output from 100 to 1000 rpm in [Watts]
Pnetfinal=cell(length(rpm),1);
for l=1:length(rpm)
      Pnetfinal{l}=max(Pnet{l},[],2);
      PnetfinalkW{l}=Pnetfinal{l}./1000;
end

% Calculation of the available effective power of the WASP system
fPeff=cell(length(rpm),1);
for t=1:1:length(rpm)
      fPeff{t}=(((Vref.*Fx{t}.*WP)./ht)-PW{t})./1000;
end

% Maximum values of the aforementioned available effective power
fPeffmax=zeros(length(Wind_angle),length(Wind_speed));
for l=1:length(rpm)
      fPeffmax=max(fPeffmax,fPeff{l});
end

% Generating the sum of the available eefctive power
sumfPeff=sum(sum(fPeffmax));

% Calculating the EEDI index
EEDI=4.225-((sumfPeff.*3.114.*170)./(15.25.*89506))
```

Appendix III

```
clear all
close all

% Rotor dimensions
Rfr=1.2;            % Radius in [meters]
Hfr=20;             % Height in [meters]
Afr=2.*Rfr.*Hfr;    % Area of the affected cross-sectional surface in
[meters^2]
Ar=2.*pi.*Rfr.*Hfr; % Surface area of the rotor in [meters^2]
rpm=[100:100:1000]; % Rotational speed of the rotor in [rpm]
rs=2.*pi.*rpm./60;  % rpm to rotations per second

% Extra constants
p=1.225;            % Air density in [kg/m^3]
ma=0.0000181;       % Air's dynamic viscosity in [kg/(m*s)]

% Ship Characteristics
Vref=7.8446;        % Ship's reference speed in [m/s]
ht=0.75;            % System's efficiency

%Lift/Drag Coefficients
% Velocity ratio
X=[0,0.5,1,1.5,2,2.5,3,3.5,4,4.5,5,5.5,6,6.5,7,7.5,8];
% Lift Coefficient
Cl=[0,0.2,1,2.5,4.2,6.15,8,9.3,10,10.3,10.9,11,11.1,11.4,11.6,11.7,11.8
];
% Drag Coefficient
Cd=[1,0.8,0.6,0.7,0.9,1.5,2,2.8,3,3.2,3.5,3.6,3.8,3.9,3.95,4,4.1];



Wind_angle=0:5:355; % True wind angle in [degrees]
Wind_speed=1:1:25;  % True wind speed in [m/s]

% Introduce apparent wind speed & angle matrices
Pv=[];
Pa=[];

% for-loop for apparent wind speed & angle
for i=1:1:length(Wind_angle)
    [V,A]=App_Wind_Speed_Angle(Wind_speed,Vref,Wind_angle(1,i));
    Pv=[Pv;V];
    Pa=[Pa;A];
end

Pa=real(Pa);                    % Keeps only the real part of the
                                  matrix

Vrot=rs.*Rfr;                   % Linear velocity on the rotor's
                                  surface in [m/s]
Re=p.*rs.*Rfr.^2.*(1./ma);      % Reynold's number
Cf=0.0576./(Re.^(1./5));        % Skin friction coefficient
```

```
Ff=0.5.*Cf.*p.*Vrot.^2.*Ar;      % Frictional force in [N]
Pcon=Ff.*Vrot;                   % Power required to rotate the rotor in
                                   [Watts]

GW=load('matlab.mat');           % Load global wind probability matrix
WP=cell2mat(struct2cell(GW));    % Transition from cell to matrix

% Introduce cells of length(rpm) by 1
Vrat=cell(length(rpm),1);        % Velocity ratio
Fl=cell(length(rpm),1);          % Lift force in [N]
Fd=cell(length(rpm),1);          % Drag force in [N]
Fx=cell(length(rpm),1);          % Effective force parallel to ship's
                                   direction in [N]
Fy=cell(length(rpm),1);          % Effective force vertically to ship's
                                   direction in [N]
Ps=cell(length(rpm),1);          % System power output in [Watts]
PW=cell(length(rpm),1);          % Power consumption * global wind
                                   probability in [Watts]
Clfun=cell(length(rpm),1);       % Lift coefficient function
Cdfun=cell(length(rpm),1);       % Drag coefficient function
Pnet=cell(length(rpm),1);        % Net power output in [Watts]

% for-loop generating data for the above cells (lines 50-60)
for k=1:1:length(rpm)

      Vrat{k}=(rs(k).*Rfr)./Pv;
      Vrat{k}=min(Vrat{k},7.61);      % Bounding the value due to the
                                        asymptotic form of the lift and
                                        drag coefficient

      % form of the lift & drag coefficient functions
      Clfun{k}=-0.0008259.*Vrat{k}.^6+0.01494.*Vrat{k}.^5-
      0.05744.*Vrat{k}.^4-0.3346.*Vrat{k}.^3+2.405.*Vrat{k}.^2-
      1.075.*Vrat{k}+0.05456;
      Cdfun{k}=-0.0007167.*Vrat{k}.^6+0.01705.*Vrat{k}.^5-
      0.1437.*Vrat{k}.^4+0.4656.*Vrat{k}.^3-0.2084.*Vrat{k}.^2-
      0.5551.*Vrat{k}+1.025;

      Fl{k}=0.5.*p.*Pv.^2.*Afr.*Clfun{k}; % Lift force function in [N]
      Fd{k}=0.5.*p.*Pv.^2.*Afr.*Cdfun{k}; % Drag force function in [N]

      % Effective force functions in [N]
      Fx{k}=Fl{k}.*sin(deg2rad(Pa))-Fd{k}.*cos(deg2rad(Pa));
      Fx{k}=real(Fx{k});
      Fx{k}=max(Fx{k},0);
      Fy{k}=Fl{k}.*cos(deg2rad(Pa))+Fd{k}.*sin(deg2rad(Pa));

      % System power output in [Watts]
      Ps{k}=Fx{k}.*Vref;
      Pnet{k}=(Ps{k}-Pcon(k)).*ht;
      Pnet{k}=max(Pnet{k},0);
      PW{k}=Pcon(k).*WP;
end
```

```
% Maximum system power output from 100 to 1000 rpm in [Watts]
Psfinal=cell(length(rpm),1);
for l=1:length(rpm)
      Psfinal{l}=max(Ps{l},[],2);
      PsfinalkW{l}=Psfinal{l}./1000;
end

% Maximum net power output from 100 to 1000 rpm in [Watts]
Pnetfinal=cell(length(rpm),1);
for l=1:length(rpm)
      Pnetfinal{l}=max(Pnet{l},[],2);
      PnetfinalkW{l}=Pnetfinal{l}./1000;
end

% Calculation of the available effective power from the WASP
fPeff=cell(length(rpm),1);
for t=1:1:length(rpm)
      fPeff{t}=(((Vref.*Fx{t}.*WP)./ht)-PW{t})./1000;
      fPeff{t}=max(fPeff{t},0);
end

% Maximum values of the aforementioned available effective power
fPeffmax=zeros(length(Wind_angle),length(Wind_speed));
for l=1:length(rpm)
      fPeffmax=max(fPeffmax,fPeff{l});
end


EEDI=cell(length(Wind_angle),1);
% Calculating the EEDI index
for s=1:length(Wind_angle)
    for i=1:length(Wind_speed)
    EEDI{s}(1,i)=4.225-((fPeffmax(s,i).*3.114.*170)./(15.25.*89506));
    end
end

% Calculating the EEDI index for fixed rpm values
(100,300,600,800,1000)
EEDI100=4.225-((sum(sum(fPeff{1})).*3.114.*170)./(15.25.*89506))
EEDI300=4.225-((sum(sum(fPeff{3})).*3.114.*170)./(15.25.*89506))
EEDI600=4.225-((sum(sum(fPeff{6})).*3.114.*170)./(15.25.*89506))
EEDI800=4.225-((sum(sum(fPeff{8})).*3.114.*170)./(15.25.*89506))
EEDI1000=4.225-((sum(sum(fPeff{10})).*3.114.*170)./(15.25.*89506))
```

Appendix IV

```
clear all
close all

% Rotor dimensions
Rfr=1.2;            % Radius in [meters]
Hfr=20;             % Height in [meters]
Afr=2.*Rfr.*Hfr;    % Area of the affected cross-sectional surface in
                      [meters^2]
Ar=2.*pi.*Rfr.*Hfr; % Surface area of the rotor in [meters^2]
rpm=[100:100:1000]; % Rotational speed of the rotor in [rpm]
rs=2.*pi.*rpm./60;  % rpm to rotations per second

% Extra constants
p=1.225;            % Air density in [kg/m^3]
ma=0.0000181;       % Air's dynamic viscosity in [kg/(m*s)]

% Ship Characteristics
Vref=7.8446;        % Ship's reference speed in [m/s]
ht=0.75;            % System's efficiency

%Lift/Drag Coefficients
% Velocity ratio
X=[0,0.5,1,1.5,2,2.5,3,3.5,4,4.5,5,5.5,6,6.5,7,7.5,8];
% Lift Coefficient
Cl=[0,0.2,1,2.5,4.2,6.15,8,9.3,10,10.3,10.9,11,11.1,11.4,11.6,11.7,11.8
];
% Drag Coefficient
Cd=[1,0.8,0.6,0.7,0.9,1.5,2,2.8,3,3.2,3.5,3.6,3.8,3.9,3.95,4,4.1];


Wind_angle=80:5:120; % True wind angle in [degrees]
Wind_speed=1:1:17;   % True wind speed in [m/s]

% Introduce apparent wind speed & angle matrices
Pv=[];
Pa=[];

% for-loop for apparent wind speed & angle
for i=1:1:length(Wind_angle)
    [V,A]=App_Wind_Speed_Angle(Wind_speed,Vref,Wind_angle(1,i));
    Pv=[Pv;V];
    Pa=[Pa;A];
end

Pa=real(Pa);                    % Keeps only the real part of the
                                  matrix

Vrot=rs.*Rfr;                   % Linear velocity on the rotor's
                                  surface in [m/s]
Re=p.*rs.*Rfr.^2.*(1./ma);      % Reynold's number
Cf=0.0576./(Re.^(1./5));        % Skin friction coefficient
```

```
Ff=0.5.*Cf.*p.*Vrot.^2.*Ar;      % Frictional force in [N]
Pcon=Ff.*Vrot;                   % Power required to rotate the rotor in
                                   [Watts]

GW=load('matlab.mat');           % Load global wind probability matrix
WP=cell2mat(struct2cell(GW));    % Transition from cell to matrix

% Normalized Global Wind Probability Matrix
WP=WP(17:25,:);
WP=WP(:,1:17);
sumWP=sum(sum(WP));
WP=WP./sumWP;

% Introduce cells of length(rpm) by 1
Vrat=cell(length(rpm),1);        % Velocity ratio
Fl=cell(length(rpm),1);          % Lift force in [N]
Fd=cell(length(rpm),1);          % Drag force in [N]
Fx=cell(length(rpm),1);          % Effective force parallel to ship's
                                   direction in [N]
Fy=cell(length(rpm),1);          % Effective force vertically to ship's
                                   direction in [N]
Ps=cell(length(rpm),1);          % System power output in [Watts]
PW=cell(length(rpm),1);          % Power consumption * global wind
                                   probability in [Watts]
Clfun=cell(length(rpm),1);       % Lift coefficient function
Cdfun=cell(length(rpm),1);       % Drag coefficient function
Pnet=cell(length(rpm),1);        % Net power output in [Watts]

% for-loop generating data for the above cells (lines 50-60)
for k=1:1:length(rpm)

      Vrat{k}=(rs(k).*Rfr)./Pv;
      Vrat{k}=min(Vrat{k},7.61);      % Bounding the value due to the
                                        asymptotic form of the lift and
                                        drag coefficient

      % form of the lift & drag coefficient functions
      Clfun{k}=-0.0008259.*Vrat{k}.^6+0.01494.*Vrat{k}.^5-
      0.05744.*Vrat{k}.^4-0.3346.*Vrat{k}.^3+2.405.*Vrat{k}.^2-
      1.075.*Vrat{k}+0.05456;
      Cdfun{k}=-0.0007167.*Vrat{k}.^6+0.01705.*Vrat{k}.^5-
      0.1437.*Vrat{k}.^4+0.4656.*Vrat{k}.^3-0.2084.*Vrat{k}.^2-
      0.5551.*Vrat{k}+1.025;

      Fl{k}=0.5.*p.*Pv.^2.*Afr.*Clfun{k}; % Lift force function in [N]
      Fd{k}=0.5.*p.*Pv.^2.*Afr.*Cdfun{k}; % Drag force function in [N]

      % Effective force functions in [N]
      Fx{k}=Fl{k}.*sin(deg2rad(Pa))-Fd{k}.*cos(deg2rad(Pa));
      Fx{k}=real(Fx{k});
      Fx{k}=max(Fx{k},0);
      Fy{k}=Fl{k}.*cos(deg2rad(Pa))+Fd{k}.*sin(deg2rad(Pa));

      % System power output in [Watts]
```

```
      Ps{k}=Fx{k}.*Vref;
      Pnet{k}=(Ps{k}-Pcon(k)).*ht;
      Pnet{k}=max(Pnet{k},0);
      PW{k}=WP.*Pcon(k);
end

% Maximum system power output from 100 to 1000 rpm in [Watts]
Psfinal=cell(length(rpm),1);
for l=1:length(rpm)
      Psfinal{l}=max(Ps{l},[],2);
      PsfinalkW{l}=Psfinal{l}./1000;
end

% Maximum net power output from 100 to 1000 rpm in [Watts]
Pnetfinal=cell(length(rpm),1);
for l=1:length(rpm)
      Pnetfinal{l}=max(Pnet{l},[],2);
      PnetfinalkW{l}=Pnetfinal{l}./1000;
end

% Calculation of the available effective power from the WASP
fPeff=cell(length(rpm),1);
for t=1:1:length(rpm)
      fPeff{t}=(((Vref.*Fx{t}.*WP)./ht)-PW{t})./1000;
      fPeff{t}=max(fPeff{t},0);
end

% Maximum values of the aforementioned available effective power
fPeffmax=zeros(length(Wind_angle),length(Wind_speed));
for l=1:length(rpm)
      fPeffmax=max(fPeffmax,fPeff{l});
end

% Generating the sum of the available eefctive power
sumfPeff=sum(sum(fPeffmax));

% Calculating the EEDI index
EEDI=4.225-((sumfPeff.*3.114.*170)./(15.25.*89506))
```

Appendix V

```
clear all
close all

% Rotor dimensions
Rfr=1.2;            % Radius in [meters]
Hfr=20;             % Height in [meters]
Afr=2.*Rfr.*Hfr;    % Area of the affected cross-sectional surface in
                      [meters^2]
Ar=2.*pi.*Rfr.*Hfr; % Surface area of the rotor in [meters^2]
rpm=[100:100:300];  % Rotational speed of the rotor in [rpm] (for 10-
                      gear Flettner rotor 300 is replaced by 1000)
rs=2.*pi.*rpm./60;  % rpm to rotations per second

% Extra constants
p=1.225;            % Air density in [kg/m^3]
ma=0.0000181;       % Air's dynamic viscosity in [kg/(m*s)]

% Ship Characteristics
Vref=7.8446;        % Ship's reference speed in [m/s]
ht=0.75;            % System's efficiency

%Lift/Drag Coefficients
% Velocity ratio
X=[0,0.5,1,1.5,2,2.5,3,3.5,4,4.5,5,5.5,6,6.5,7,7.5,8];
% Lift Coefficient
Cl=[0,0.2,1,2.5,4.2,6.15,8,9.3,10,10.3,10.9,11,11.1,11.4,11.6,11.7,11.8
];
% Drag Coefficient
Cd=[1,0.8,0.6,0.7,0.9,1.5,2,2.8,3,3.2,3.5,3.6,3.8,3.9,3.95,4,4.1];

Wind_angle=[75,90,115]; % True wind angle in [degrees]
Wind_speed=5:2.5:20;  % True wind speed in [m/s]

% Introduce apparent wind speed & angle matrices
Pv=[];
Pa=[];

% for-loop for apparent wind speed & angle
for i=1:1:length(Wind_angle)
    [V,A]=App_Wind_Speed_Angle(Wind_speed,Vref,Wind_angle(1,i));
    Pv=[Pv;V];
    Pa=[Pa;A];
end

Pa=real(Pa);                    % Keeps only the real part of the
                                  matrix

Vrot=rs.*Rfr;                   % Linear velocity on the rotor's
                                  surface in [m/s]
Re=p.*rs.*Rfr.^2.*(1./ma);      % Reynold's number
Cf=0.0576./(Re.^(1./5));        % Skin friction coefficient
Ff=0.5.*Cf.*p.*Vrot.^2.*Ar;     % Frictional force in [N]
```

```
Pcon=Ff.*Vrot;                  % Power required to rotate the rotor in
                                  [Watts]

% The wind probability matrix is 1 because the wind conditions are
constant
WP=1;

% Introduce cells of length(rpm) by 1
Vrat=cell(length(rpm),1);       % Velocity ratio
Fl=cell(length(rpm),1);         % Lift force in [N]
Fd=cell(length(rpm),1);         % Drag force in [N]
Fx=cell(length(rpm),1);         % Effective force parallel to ship's
                                  direction in [N]
Fy=cell(length(rpm),1);         % Effective force vertically to ship's
                                  direction in [N]
Ps=cell(length(rpm),1);         % System power output in [Watts]
PW=cell(length(rpm),1);         % Power consumption * global wind
                                  probability in [Watts]
Clfun=cell(length(rpm),1);      % Lift coefficient function
Cdfun=cell(length(rpm),1);      % Drag coefficient function
Pnet=cell(length(rpm),1);       % Net power output in [Watts]

% for-loop generating data for the above cells (lines 50-60)
for k=1:1:length(rpm)

      Vrat{k}=(rs(k).*Rfr)./Pv;
      Vrat{k}=min(Vrat{k},7.61);      % Bounding the value due to the
                                        asymptotic form of the lift and
                                        drag coefficient


      % form of the lift & drag coefficient functions
      Clfun{k}=-0.0008259.*Vrat{k}.^6+0.01494.*Vrat{k}.^5-
      0.05744.*Vrat{k}.^4-0.3346.*Vrat{k}.^3+2.405.*Vrat{k}.^2-
      1.075.*Vrat{k}+0.05456;
      Cdfun{k}=-0.0007167.*Vrat{k}.^6+0.01705.*Vrat{k}.^5-
      0.1437.*Vrat{k}.^4+0.4656.*Vrat{k}.^3-0.2084.*Vrat{k}.^2-
      0.5551.*Vrat{k}+1.025;

      Fl{k}=0.5.*p.*Pv.^2.*Afr.*Clfun{k}; % Lift force function in [N]
      Fd{k}=0.5.*p.*Pv.^2.*Afr.*Cdfun{k}; % Drag force function in [N]

      % Effective force functions in [N]
      Fx{k}=Fl{k}.*sin(deg2rad(Pa))-Fd{k}.*cos(deg2rad(Pa));
      Fx{k}=real(Fx{k});
      Fx{k}=max(Fx{k},0);
      Fy{k}=Fl{k}.*cos(deg2rad(Pa))+Fd{k}.*sin(deg2rad(Pa));

      % System power output in [Watts]
      Ps{k}=Fx{k}.*Vref;
      Pnet{k}=(Ps{k}-Pcon(k)).*ht;
      Pnet{k}=max(Pnet{k},0);
      PW{k}=Pcon(k).*WP;
end
```

```
% Maximum system power output from 100 to 1000 rpm in [Watts]
Psfinal=cell(length(rpm),1);
for l=1:length(rpm)
      Psfinal{l}=max(Ps{l},[],2);
      PsfinalkW{l}=Psfinal{l}./1000;
end

% Maximum net power output from 100 to 1000 rpm in [Watts]
Pnetfinal=cell(length(rpm),1);
for l=1:length(rpm)
      Pnetfinal{l}=max(Pnet{l},[],2);
      PnetfinalkW{l}=Pnetfinal{l}./1000;
end

% Calculation of the available effective power from the WASP
fPeff=cell(length(rpm),1);
for t=1:1:length(rpm)
      fPeff{t}=(((Vref.*Fx{t}.*WP)./ht)-PW{t})./1000;
      fPeff{t}=max(fPeff{t},0);
end

% Maximum values of the aforementioned available effective power
fPeffmax=zeros(length(Wind_angle),length(Wind_speed));
for l=1:length(rpm)
      fPeffmax=max(fPeffmax,fPeff{l});
end

EEDI=cell(length(Wind_angle),1);
% Calculating the EEDI index
for s=1:length(Wind_angle)
    for i=1:length(Wind_speed)
    EEDI{s}(1,i)=4.225-((fPeffmax(s,i).*3.114.*170)./(15.25.*89506));
    end
end

% Plotting the EEDI indices
plot(Wind_speed,EEDI{1},Wind_speed,EEDI{2},Wind_speed,EEDI{3})
```